INTERNATIONAL JOURNAL OF
NUMERICAL ANALYSIS AND MODELING
Volume 20, Number 5, Pages 618–646

doi: 10.4208/ijnam2023-1027

A POSTERIORI ERROR ANALYSIS FOR AN ULTRA-WEAK DISCONTINUOUS GALERKIN APPROXIMATIONS OF NONLINEAR SECOND-ORDER TWO-POINT BOUNDARY-VALUE PROBLEMS

MAHBOUB BACCOUCH

This paper is dedicated to the memory of my mother, Rehah Jetlaoui, who died unexpectedly in July 31, 2021 during the completion of the first part of this work [7].

Abstract. In this paper, we present and analyze *a posteriori* error estimates in the L^2-norm of an ultra-weak discontinuous Galerkin (UWDG) method for nonlinear second-order boundary-value problems for ordinary differential equations of the form $u'' = f(x, u)$. We first use the superconvergence results proved in the first part of this paper (*J. Appl. Math. Comput.* 69, 1507-1539, 2023) to prove that the UWDG solution converges, in the L^2-norm, towards a special p-degree interpolating polynomial, when piecewise polynomials of degree at most $p \geq 2$ are used. The order of convergence is proved to be $p + 2$. We then show that the UWDG error on each element can be divided into two parts. The dominant part is proportional to a special $(p+1)$-degree Baccouch polynomial, which can be written as a linear combination of Legendre polynomials of degrees $p - 1$, p, and $p + 1$. The second part converges to zero with order $p + 2$ in the L^2-norm. These results allow us to construct *a posteriori* UWDG error estimates. The proposed error estimates are computationally simple and are obtained by solving a local problem with no boundary conditions on each element. Furthermore, we prove that, for smooth solutions, these *a posteriori* error estimates converge to the exact errors in the L^2-norm under mesh refinement. The order of convergence is proved to be $p + 2$. Finally, we prove that the global effectivity index converges to unity at $\mathcal{O}(h)$ rate. Numerical results are presented exhibiting the reliability and the efficiency of the proposed error estimator.

Key words. Second-order boundary-value problems, ultra-weak discontinuous Galerkin method, superconvergence, *a posteriori* error estimation, Baccouch polynomials.

1. Introduction

This paper is a continuation of our recent paper [7] and is devoted to the *a posteriori* error estimation for the following nonlinear second-order two-point boundary-value problems (BVPs) [4, 9, 15, 18] solved with the ultra-weak discontinuous Galerkin (UWDG) method

$$u'' = f(x, u), \quad x \in \Omega = [a, b], \tag{1a}$$

$$u(a) = u_a, \quad u'(b) = u_b, \tag{1b}$$

where $f : [a, b] \times \mathbb{R} \to \mathbb{R}$ is a given smooth function. Precise conditions on f are specified later. We would like to point out that, in the present work, we restrict ourselves to either the mixed Dirichlet-Neumann boundary conditions ($u(a) = u_a$, $u'(b) = u_b$) or periodic boundary conditions ($u(a) = u(b)$, $u'(a) = u'(b)$) to simplify the presentation. The main novelty of this paper is to construct *a posteriori* error estimates of the UWDG method proposed in the first part and to prove the convergence of the proposed error estimators in the L^2-norm.

Received by the editors on December 19, 2022 and, accepted on June 30, 2023.
2000 *Mathematics Subject Classification.* 65L10, 65L60, 65L70.

Various numerical methods have been proposed to solve nonlinear differential equations in literature, such as the finite difference methods, the time-splitting pseudo-spectral methods, the finite element methods, and the discontinuous Galerkin (DG) methods, to name a few. The main reason for us to establish DG methods is because of its flexibility in handling geometry, exhibiting superconvergence properties, accommodating *hp*-adaptivity, and high parallel efficiency. The DG method was first proposed by Reed and Hill in 1973 [19] for approximating the scalar neutron equation. This type of finite element method uses a piecewise polynomial basis for both the numerical and test function, and it was originally designed to deal with the first spatial derivative only (see, *e.g.*, [11, 12, 14, 19] for detailed discussions). The original DG method has been developed in several directions over the past few decades. For instance, Cockburn and Shu [13] proposed the so-called local discontinuous Galerkin (LDG) method to solve a wide class of nonlinear convection-diffusion equations with high-order spatial derivatives. By introducing auxiliary variables that reduce the original problem into a lower-order system, typically with first-order spatial derivatives, the LDG methods ensure the stability of the scheme by suitable numerical fluxes embedded with the resulting system. See [17, 25, 26] and references therein for recent developments of the LDG method.

Another streamline of development is motivated by the urge to solve high-order problems, and this includes the ultra-weak discontinuous Galerkin method (UWDG) introduced by Despres [16] for linear elliptic PDEs. The idea of the UWDG method for higher-order equations is to shift all the spatial derivatives through integration by parts to the test function in the weak formulation, and the stability of the scheme is guaranteed by certain numerical fluxes and additional internal penalty terms when necessary.

In recent years, the study of superconvergence and *a posteriori error* estimates of DG methods has been an active research field in numerical analysis, see the monographs by Verfürth [23], Wahlbin [24], and Babuška and Strouboulis [5]. A knowledge of superconvergence properties can be used to (*i*) construct simple and asymptotically exact *a posteriori* estimates of discretization errors and (*ii*) help detect discontinuities to find elements needing limiting, stabilization and/or refinement. *A posteriori* error estimates play an essential role in assessing the reliability of numerical solutions and in developing efficient adaptive algorithms. Typically, *a posteriori* error estimators employ the known numerical solution to derive estimates of the actual solution errors. They are also used to steer adaptive schemes where either the mesh is locally refined (h-refinement) or the polynomial degree is raised (p-refinement). For an introduction to the subject of *a posteriori* error estimation see the monograph of Ainsworth and Oden [3].

In [7], we presented and analyzed a superconvergent UWDG method for the model problem (1). We first used a suitable choice of the numerical fluxes to derive optimal L^2-error estimates of the scheme. The order of convergence is proved to be $p+1$ in the L^2-norm, when piecewise polynomials of degree $p \geq 2$ are used. Moreover, we proved that the UWDG solution is superconvergent with order $p+2$ for $p = 2$ and $p+3$ for $p \geq 3$ towards a special projection of the exact solution. Finally, we proved that the UWDG solution and its derivative are superconvergent at the nodes with an order of $\mathcal{O}(h^{2p})$. Our proofs are valid for arbitrary regular meshes using piecewise polynomials with degree $p \geq 2$. Numerical experiments were presented to confirm the sharpness of all the theoretical findings. In this work, we use the results in the first part to construct efficient and reliable *a posteriori* error estimates for the UWDG method. We further prove that the proposed *a*

posteriori error estimators converge to the true errors in the L^2-norm under mesh refinement at the optimal rate. To the author's knowledge, *a posteriori* error analysis for UWDG approximations of nonlinear second-order two-point boundary-value problems has not been studied in the literature.

In this paper, we present and analyze an implicit *a posteriori* UWDG error estimate for the model BVP (1). We use the results of the first part of this work to prove that the dominant part of the spatial discretization error for the UWDG solution is proportional to a $(p+1)$-degree polynomial, when piecewise polynomials of degree at most p are used. This polynomial can be written as a linear combination of Legendre polynomials of degrees $p-1$, p, and $p+1$. We use this result to construct a residual-based *a posteriori* error estimate for the spatial error. The leading term of the discretization error is estimated by solving a local problem with no boundary conditions on each element. We further prove that the proposed UWDG error estimate converges to the true error at $\mathcal{O}(h^{p+2})$ rate. Finally, we prove that the global effectivity index in the L^2-norm converges to unity at $\mathcal{O}(h)$ rate. Our proofs are valid for any regular meshes and using piecewise polynomials of degree $p \geq 2$.

This paper is organized as follows. In Section 2, we recall the UWDG method for the second-order BVP (1). We also introduce some basic notations and preliminaries which will be used later. In Section 3, we present new superconvergence results. We present our *a posteriori* error estimation procedure and prove that these error estimates converge to the true errors under mesh refinement in L^2-norm with optimal convergence rate in Section 4. Numerical examples are provided to show the accuracy and capability of the scheme in Section 5. Some concluding remarks and future work are given in Section 6.

2. The UWDG method and Preliminaries

Since this paper is a continuation of the author's recent work [7], we adopt the same definitions and notation given therein.

2.1. The UWDG scheme. We discretize the computational interval $\Omega = [a, b]$ by non-overlapping intervals $I_i = (x_{i-1}, x_i),\ i = 1, 2, \ldots, N$ such that

$$a = x_0 < x_1 < \cdots < x_N = b.$$

Let us define the length of I_i as $h_i = x_i - x_{i-1}$. We use $h = \max\limits_{1\leq i\leq N} h_i$ and $h_{min} = \min\limits_{1\leq i\leq N} h_i$ to denote the length of the largest and smallest intervals, respectively. We assume that mesh is regular in the sense that there exists a positive constant λ such that $\lambda h \leq h_{min} \leq h$.

We denote by $v(x_i^+)$ and $v(x_i^-)$ the values of v at the discontinuity point x_i from the right cell I_{i+1} and from the left cell I_i, respectively, *i.e.*,

$$v(x_i^{\pm}) = \lim_{s\to 0^{\pm}} v(x_i + s), \quad i = 0, 1, \ldots, N.$$

Let the finite element space be the discontinuous piecewise polynomials space $V_h^p = \{v \in L^2(\Omega) :\ v|_{I_i} \in \mathbb{P}^p(I_i),\ i = 1, 2, \ldots, N\}$, where $\mathbb{P}^p(I_i)$ is the set of polynomials of degree up to $p \geq 0$ defined on the interval I_i.

Multiplying (1a) by a test function v, integrating over an arbitrary interval I_i, and using integration by parts twice, we get the following UWDG weak formulation

$$\int_{I_i} (-u\ v'' + v f(x,u))\ dx - u'(x_i)v(x_i) + u'(x_{i-1})v(x_{i-1}) + u(x_i)v'(x_i) - u(x_{i-1})v'(x_{i-1}) = 0. \tag{2}$$

Next, we use the UWDG weak formulation (2) to define the UWDG scheme as follows: We approximate u by $u_h \in V_h^p$ and we choose the test function $v \in V_h^p$ to get the following UWDG scheme: Find $u_h \in V_h^p$ such that for all $v \in V_h^p$

$$\begin{aligned}&\int_{I_i} (-u_h v'' + v f(x,u_h))\, dx - \widehat{u_h'}(x_i)v(x_i^-) + \widehat{u_h'}(x_{i-1})v(x_{i-1}^+)\\ &+ \widehat{u_h}(x_i)v'(x_i^-) - \widehat{u_h}(x_{i-1})v'(x_{i-1}^+) = 0,\end{aligned} \tag{3a}$$

holds for all $i = 1, 2, \ldots, N$. In (3a), we used the hat terms $\widehat{u_h}$ and $\widehat{u_h'}$ to denote the so-called numerical fluxes, which are nothing but approximations to u and u' at the node x_i, respectively. We would like to emphasize that the choice of the numerical fluxes $\widehat{u_h}$ and $\widehat{u_h'}$ is crucial for the accuracy of the UWDG method.

To complete the UWDG scheme, we need to specify the numerical fluxes $\widehat{u_h}$ and $\widehat{u_h'}$. In this paper, when the mixed boundary conditions (1b) are used, we choose the following alternating numerical fluxes

(3b)

$$\widehat{u_h}(x_i) = \begin{cases} u_a, & i = 0,\\ u_h(x_i^-), & i = 1, 2, \ldots, N, \end{cases} \quad \widehat{u_h'}(x_i) = \begin{cases} u_h'(x_i^+), & i = 0, 1, \ldots, N-1,\\ u_b, & i = N. \end{cases}$$

When the periodic boundary conditions are used, we use

$$\widehat{u_h}(x_i) = u_h(x_i^-), \quad \widehat{u_h'}(x_i) = u_h'(x_i^+), \quad i = 0, 1, \ldots, N. \tag{3c}$$

After we select the numerical fluxes, the resulting finite dimensional problem becomes an algebraic system of nonlinear equations to which the Newton-Rapshon iterative scheme can be applied to find the unknown coefficients in u_h.

2.2. Norms. Throughout this paper, we adopt the following notation

- Let $(u, v)_{I_i} = \int_{I_i} u(x)v(x)\, dx$ be the standard L^2-inner product over the interval I_i.
- Denote $\|u\|_{0,I_i} = (u,u)_{I_i}^{1/2} = \left(\int_{I_i} u^2(x)dx\right)^{1/2}$ to be the standard L^2-norm of u on I_i.
- For any natural number ℓ, we use $H^\ell(I_i) = \left\{u \in L^2(I_i) :\ D^k u \in L^2(I_i),\ \forall\ k \le \ell\right\}$ to denote the standard Sobolev space on I_i, where $D^k u = \frac{d^k u}{dx^k}$.
- The H^ℓ-norm of a real-valued function $u \in H^\ell(I_i)$ on the interval I_i is defined by

$$\|u\|_{\ell,I_i} = \left(\sum_{k=1}^{\ell} \left\|D^k u\right\|_{0,I_i}^2\right)^{1/2}.$$

- The broken Sobolev H^ℓ-norm of u on the whole domain Ω by

$$\|u\| = \left(\sum_{i=1}^{N} \|u\|_{0,I_i}^2\right)^{1/2}, \quad \|u\|_\ell = \left(\sum_{i=1}^{N} \|u\|_{\ell,I_i}^2\right)^{1/2}, \quad \ell = 1, 2, \ldots.$$

- The semi-norm on the element I_i and the semi-norm on the computational domain Ω as

$$|u|_{\ell,I_i} = \left\|D^\ell u\right\|_{0,I_i}, \quad |u|_\ell = \left(\sum_{i=1}^{N} |u|_{\ell,I_i}^2\right)^{1/2}.$$

2.3. Projections. For any given function $u(x) \in H^{p+1}(\Omega)$ and $p \geq 1$, we define the projection $P_h^- u$ by the following conditions

(4)
$$\int_{I_i} (u - P_h^- u) v \, dx = 0, \ \forall \ v \in \mathbb{P}^{p-2}(I_i), \ (u - P_h^- u)'(x_{i-1}^+) = 0, \ (u - P_h^- u)(x_i^-) = 0.$$

Similarly, the projection P_h^+ satisfies

(5)
$$\int_{I_i} (u - P_h^+ u) v \, dx = 0, \ \forall \ v \in \mathbb{P}^{p-2}(I_i), \ (u - P_h^+ u)(x_{i-1}^+) = 0, \ (u - P_h^+ u)'(x_{i-1}^+) = 0.$$

By a standard scaling argument together with the trace inequality [10, 22], we have the following *a priori* error estimates

$$\left\| u - P_h^{\pm} u \right\| + h \left\| u - P_h^{\pm} u \right\|_{\infty} + h^{1/2} \left\| u - P_h^{\pm} u \right\|_{\Gamma_h} \leq C h^{p+1} \left\| u \right\|_{p+1}, \tag{6}$$

where C is a positive constant dependent on p but not on h, Γ_h denotes the set of boundary points of all elements I_i, and $\|v\|_{\Gamma_h}^2 = \sum_{i=1}^{N} \left(v^2(x_{i-1}^+) + v^2(x_i^-) \right)$.

2.4. Inverse properties. We summarize the classical inverse properties of the finite element space V_h^p in the following lemma [10].

Lemma 2.1. *If $v \in V_h^p$ then there exists a positive constant C independent of the mesh size h such that*

$$\left\| v' \right\| \leq C h^{-1} \left\| v \right\|, \quad \left\| v \right\|_{\infty} \leq C h^{-1/2} \left\| v \right\|, \quad \left\| v \right\|_{\Gamma_h} \leq C h^{-1/2} \left\| v \right\|. \tag{7}$$

For the rest of the paper, we denote by C (with or without superscripts or subscripts) a generic positive constant which is independent of the step size h, but depend on the exact solution of the model problem (1). Furthermore, it may vary from line to line.

2.5. A priori error estimates and superconvergence results. In this section, we summarize the error estimates in the L^2-norm and superconvergence results proved in the first part, which will be needed in our *a posteriori* error analysis. We first impose the following assumptions on the function $f(x,u): \ [a,b] \times \mathbb{R} \to \mathbb{R}$

(1) $f(x,u)$ and $\frac{\partial f(x,u)}{\partial u}$ are continuous functions on the set $D = \{(x,u) \mid x \in [a,b], \ u \in \mathbb{R}\}$.
(2) There exists a positive constant L such that

$$\left| \frac{\partial f(x,u)}{\partial u} \right| \leq L, \quad \text{for all } (x,u) \in D. \tag{8}$$

By the Mean-Value Theorem, the function f satisfies the following uniform Lipschitz condition on D in the variable u with uniform Lipschitz constant L

$$|f(x,u) - f(x,v)| \leq L \, |u - v|, \quad \text{for all } (x,u), \ (x,v) \in D = [a,b] \times \mathbb{R}. \tag{9}$$

Let $e_u = u - u_h$ be the error between the exact and numerical solutions. Then, we decompose the actual error into two terms as

$$e_u = \xi_u + \eta_u, \tag{10}$$

where $\xi_u = P_h^- u - u_h \in V_h^p$ is the error between the UWDG solution and the projection of the exact solution and $\eta_u = u - P_h^- u$ is the projection error.

We are now ready to present error estimates for the UWDG scheme.

Theorem 2.1. *Suppose that $u \in H^{p+1}(\Omega)$ solves (1). Let $p \geq 2$ and u_h be the UWDG solution defined in (3). Then, for sufficiently small h, we have*

$$\|e_u\| \leq Ch^{p+1}, \tag{11}$$

$$\|e_u\|_\infty \leq Ch^p, \tag{12}$$

where C is a positive constant independent of the mesh size h.

Proof. See [7, Theorem 3.1]. □

Next, we recall an important superconvergence result towards the projection $P_h^- u$.

Theorem 2.2. *Suppose that the assumptions of Theorem 2.1 are satisfied. We further assume that the function $g(x) = \frac{\partial f(x,u(x))}{\partial u}$ is a sufficiently smooth function satisfying $\left|\frac{d^k g(x)}{dx^k}\right| \leq C$ for $k = 1, 2$. Then there exists a positive constant C independent of h such that*

$$\|\xi_u\| \leq \begin{cases} Ch^{p+2}, & p = 2, \\ Ch^{p+3}, & p \geq 3. \end{cases} \tag{13}$$

Proof. See [7, Theorem 4.1]. □

Finally, we recall the pointwise superconvergence at the downwind and upwind points and for the cell averages.

Theorem 2.3. *Assume that the assumptions of Theorem 2.2 are satisfied. In addition, we assume that $g(x) = \frac{\partial f(x,u(x))}{\partial u}$ is sufficiently smooth function. To be more precise, we assume that the function $g(x) \in C^p(\Omega)$. Then there exists a positive constant C such that*

$$\left|e_u(x_k^-)\right| \leq Ch^{2p}, \quad \left|e_u'(x_{k-1}^+)\right| \leq Ch^{2p}, \quad k = 1, 2, \ldots, N. \tag{14}$$

$$\left(\frac{1}{N}\sum_{k=1}^{N}\left|e_u(x_k^-)\right|^2\right)^{1/2} \leq Ch^{2p+\frac{1}{2}}, \quad \left(\frac{1}{N}\sum_{k=1}^{N}\left|e_u'(x_{k-1}^+)\right|^2\right)^{1/2} \leq Ch^{2p+\frac{1}{2}}. \tag{15}$$

Proof. See [7, Theorems 4.2 and 4.3]. □

3. Superconvergence towards a special interpolating polynomial

Here, we use the previous results to show that the true error e_u can be divided into a dominant part and a less dominant part. The dominant part is proportional to the $(p+1)$-degree polynomial and the less dominant part converges at $\mathcal{O}(h^{p+2})$ rate in the L^2-norm.

3.1. Jacobi polynomials. In our analysis, we will use the classical Jacobi polynomial defined by the Rodgrigues formula [1]

$$\hat{P}_k^{\alpha,\beta}(\xi) = \frac{(-1)^k}{2^k k!}(1-\xi)^{-\alpha}(1+\xi)^{-\beta}\frac{d^k}{d\xi^k}\left[(1-\xi)^{\alpha+k}(1+\xi)^{\beta+k}\right], \tag{16}$$
$$\alpha, \beta > -1, \ k = 0, 1, 2, \ldots,$$

for $\xi \in [-1, 1]$. We note that if $\alpha = \beta = 0$, then it reduces to the kth-degree Legendre polynomial, which will be denoted by $\hat{L}_k(\xi) = \hat{P}_k^{0,0}(\xi)$ on $[-1, 1]$.

The kth-degree Legendre polynomial, $\hat{L}_k(\xi) = \hat{P}_k^{0,0}(\xi)$ on $[-1,1]$, satisfies the following properties:

$$\hat{L}_k(1) = 1, \quad \hat{L}_k'(1) = \frac{k(k+1)}{2}. \tag{17a}$$

$$\hat{L}_k(-\xi) = (-1)^k \hat{L}_k(\xi). \tag{17b}$$

$$\hat{L}_k'(-1) = (-1)^{k+1} \frac{k(k+1)}{2}. \tag{17c}$$

The results in (17a) and (17b) can be found in [1]. To show (17c), we differentiate (17b) with respect to ξ to get $-\hat{L}_k'(-\xi) = (-1)^k \hat{L}_k'(\xi)$. Setting $\xi = 1$ and using (17a), we obtain

$$\hat{L}_k'(-1) = (-1)^{k+1} \hat{L}_k'(1) = (-1)^{k+1} \frac{k(k+1)}{2}.$$

Next, we define the k-degree right Radau polynomial on $[-1,1]$ as (see [2])

$$\tilde{R}_k(\xi) = (\xi - 1)\hat{P}_{k-1}^{1,0}(\xi) = \tilde{L}_k(\xi) - \tilde{L}_{k-1}(\xi), \ -1 \le \xi \le 1, \tag{18}$$

which has k real distinct roots, $-1 < r_1 < r_2 < \cdots < r_k = 1$.

We further note Jacobi polynomials satisfy the orthogonality condition [1]

$$\int_{-1}^{1} (1-\xi)^\alpha (1+\xi)^\beta \hat{P}_k^{\alpha,\beta}(\xi) \hat{P}_l^{\alpha,\beta}(\xi) d\xi = \gamma_k \delta_{kl}, \quad \alpha, \beta > -1, \tag{19}$$

where $\gamma_k = \frac{2^{\alpha+\beta+1}}{2k+\alpha+\beta+1} \frac{\Gamma(k+\alpha+1)\Gamma(k+\beta+1)}{k!\Gamma(k+\alpha+\beta+1)} > 0$ and δ_{kl} is the Kronecker symbol equal to 1 if $k = l$ and 0, otherwise. Here, $\Gamma(x) = \int_0^\infty t^{x-1} e^{-t}\, dt$ is the classical Gamma function.

We also need the coefficient of the term ξ^k in $\hat{P}_k^{\alpha,\beta}(\xi)$, which is given by (see [1])

$$A_k = \frac{\Gamma(2k+\alpha+\beta+1)}{2^k k! \Gamma(k+\alpha+\beta+1)}. \tag{20}$$

Mapping the physical element I_i into the reference element $[-1,1]$ by the standard affine mapping

$$x = \frac{x_i + x_{i-1}}{2} + \frac{h_i}{2}\xi, \tag{21}$$

we get the k-degree shifted Jacobi polynomial $P_{k,i}^{\alpha,\beta}(x)$, the k-degree shifted Legendre polynomial $L_{k,i}(x)$, and the k-degree shifted right Radau polynomial $R_{k,i}(x)$ on I_i

$$P_{k,i}^{\alpha,\beta}(x) = \hat{P}_k^{\alpha,\beta}\left(\frac{2x - x_i - x_{i-1}}{h_i}\right),$$
$$L_{k,i}(x) = P_{k,i}^{0,0}(x), \quad R_{k,i}(x) = L_{k,i}(x) - L_{k-1,i}(x).$$

3.2. Baccouch polynomials. Before we state the main superconvergence results, we define some special polynomials, which, to the best of our knowledge, are not defined in the literature. Since these polynomials play an important role in our *a posteriori* error analysis, we name them after the author's last name.

Definition 3.1 (Baccouch polynomials)**.** *The Baccouch polynomials, denoted by* $\hat{B}_k(\xi)$*, are defined by* $\hat{B}_0(\xi) = 1$*,* $\hat{B}_1(\xi) = 1 - \xi$*, and, for* $k \geq 2$*, by the recurrence relation*

$$\hat{B}_k(\xi) = \hat{L}_k(\xi) - \hat{L}_{k-1}(\xi) + \frac{k^2}{(k-1)^2}\left(\hat{L}_{k-1}(\xi) - \hat{L}_{k-2}(\xi)\right), \quad -1 \leq \xi \leq 1. \tag{22}$$

We remark that $\hat{B}_k(\xi)$ can be written in terms of right-Radau and Jacobi polynomials as

$$\hat{B}_k(\xi) = \hat{R}_k(\xi) + \frac{k^2}{(k-1)^2}\hat{R}_{k-1}(\xi) \tag{23a}$$

$$= (\xi - 1)\hat{P}^{1,0}_{k-1}(\xi) + \frac{k^2}{(k-1)^2}(\xi - 1)\hat{P}^{1,0}_{k-2}(\xi), \quad -1 \leq \xi \leq 1. \tag{23b}$$

The first seven Baccouch polynomials and their roots are given in Table 1 and Table 2.

TABLE 1. The first seven Baccouch polynomials.

k	$\hat{B}_k(\xi)$
0	1
1	$1-\xi$
2	$\frac{3}{2}(-3+2\xi+\xi^2)$
3	$\frac{5}{8}(-1-6\xi+3\xi^2+4\xi^3)$
4	$\frac{7}{72}(13-12\xi-66\xi^2+20\xi^3+45\xi^4)$
5	$\frac{9}{128}(3+60\xi-30\xi^2-180\xi^3+35\xi^4+112\xi^5)$
6	$\frac{11}{400}(-31+30\xi+435\xi^2-140\xi^3-945\xi^4+126\xi^5+525\xi^6)$
7	$\frac{13}{576}(-5-210\xi+105\xi^2+1400\xi^3-315\xi^4-2394\xi^5+231\xi^6+1188\xi^7)$

TABLE 2. The roots of first seven Baccouch polynomials.

k	Roots of $\hat{B}_k(\xi)$
1	1
2	-3, 1
3	-1.59307, -0.15693, 1
4	-1.2874, -0.558689, 0.401648, 1
5	-1.17026, -0.730541, -0.0491512, 0.637447, 1
6	-1.11277, -0.818813, -0.327203, 0.261555, 0.757236, 1
7	-1.08026, -0.86995, -0.503043, -0.0236188, 0.456239,0.826185, 1

Lemma 3.1. *The polynomial* $\hat{B}_k(\xi)$ *satisfies the following properties*

$$\hat{B}_k(1) = 0, \quad \hat{B}'_k(-1) = 0, \quad k \geq 2, \tag{24}$$

$$\int_{-1}^{1} \hat{B}_k(\xi)v(\xi)\,d\xi = 0, \quad \forall\ v \in \mathbb{P}^{k-3}([-1,1]), \quad k \geq 3. \tag{25}$$

Furthermore, $\hat{B}_k(\xi)$ *has* k *distinct real roots* $b_0, b_1, \ldots, b_{k-1}$*, where* $b_0 < -1$*, the* $k-1$ *roots* $b_1 < b_2 < \cdots < b_{k-2}$ *lie in* $(-1,1)$*, and* $b_{k-1} = 1$*. Finally, we have*

$$\hat{B}_k(\xi) = \frac{(2k)!}{2^k(k!)^2}\prod_{j=0}^{k-1}(\xi - b_j). \tag{26}$$

Proof. Since $\hat{L}_k(1) = 1$, (22) gives $\hat{B}_k(1) = 0$. Next, we use (17c) to get

$$\begin{aligned}
\hat{B}'_k(-1) &= \hat{L}'_k(-1) - \hat{L}'_{k-1}(-1) + \frac{k^2}{(k-1)^2}\left(\hat{L}'_{k-1}(-1) - \hat{L}'_{k-2}(-1)\right) \\
&= (-1)^{k+1}\frac{k(k+1)}{2} - (-1)^k\frac{(k-1)k}{2} + (-1)^k\frac{k^2(k-1)}{(k-1)^2}\left(\frac{k}{2} + \frac{k-2}{2}\right) \\
&= \frac{(-1)^{k+1}}{2}\left[k(k+1) + (k-1)k - 2k^2\right] \\
&= 0.
\end{aligned}$$

The proof of (25) follows immediately from the orthogonality relation $\int_{-1}^{1} \hat{L}_k(\xi)v(\xi)\,d\xi = 0$, $\forall\ v \in \mathbb{P}^{k-1}([-1,1])$.

Next, we show that $\hat{B}_k(\xi)$ has k distinct real roots $b_0, b_1, \ldots, b_{k-1}$, where $b_0 < -1$, the $k-1$ roots $b_1 < b_2 < \cdots < b_{k-2}$ lie in $(-1,1)$, and $b_{k-1} = 1$. Using (16) with $\alpha = 1$ and $\beta = 0$, we have

$$\begin{aligned}
\hat{P}^{1,0}_{k-1}(\xi) &= \frac{(-1)^{k-1}}{2^{k-1}(k-1)!}(1-\xi)^{-1}\frac{d^{k-1}}{d\xi^{k-1}}\left[(1-\xi)^k(1+\xi)^{k-1}\right], \\
\hat{P}^{1,0}_{k-2}(\xi) &= \frac{(-1)^{k-2}}{2^{k-2}(k-2)!}(1-\xi)^{-1}\frac{d^{k-2}}{d\xi^{k-2}}\left[(1-\xi)^{k-1}(1+\xi)^{k-2}\right].
\end{aligned}$$

Combining these with (23), we get

$$\begin{aligned}
\tilde{B}_k(\xi) =& (\xi-1)\hat{P}^{1,0}_{k-1}(\xi) + \frac{k^2}{(k-1)^2}(\xi-1)\hat{P}^{1,0}_{k-2}(\xi) \\
=& (\xi-1)\frac{(-1)^{k-1}}{2^{k-1}(k-1)!}(1-\xi)^{-1}\frac{d^{k-1}}{d\xi^{k-1}}\left[(1-\xi)^k(1+\xi)^{k-1}\right] \\
&+ \frac{k^2}{(k-1)^2}(\xi-1)\frac{(-1)^{k-2}}{2^{k-2}(k-2)!}(1-\xi)^{-1}\frac{d^{k-2}}{d\xi^{k-2}}\left[(1-\xi)^{k-1}(1+\xi)^{k-2}\right] \\
=& \frac{(-1)^k}{2^{k-1}(k-1)!}\frac{d^{k-1}}{d\xi^{k-1}}\left[(1-\xi)^k(1+\xi)^{k-1}\right] \\
&+ \frac{k^2}{(k-1)^2}\frac{(-1)^{k-1}}{2^{k-2}(k-2)!}\frac{d^{k-2}}{d\xi^{k-2}}\left[(1-\xi)^{k-1}(1+\xi)^{k-2}\right] \\
=& \frac{1}{2^{k-1}(k-1)!}\frac{d^{k-1}}{d\xi^{k-1}}\left[(\xi-1)^k(1+\xi)^{k-1}\right] \\
&+ \frac{k^2}{(k-1)^2}\frac{1}{2^{k-2}(k-2)!}\frac{d^{k-2}}{d\xi^{k-2}}\left[(\xi-1)^{k-1}(1+\xi)^{k-2}\right],
\end{aligned}$$

which can be written as

$$\begin{aligned}\tilde{B}_k(\xi) =& \frac{1}{2^{k-2}(k-2)!}\frac{d^{k-2}}{d\xi^{k-2}}\left[\frac{1}{2(k-1)}\frac{d}{d\xi}\left[(\xi-1)^k(1+\xi)^{k-1}\right]\right.\\ &\left.+\frac{k^2}{(k-1)^2}(\xi-1)^{k-1}(1+\xi)^{k-2}\right]\\ =& \frac{1}{2^{k-2}(k-2)!}\frac{d^{k-2}}{d\xi^{k-2}}\left[\frac{k(\xi-1)^{k-1}(1+\xi)^{k-1}}{2(k-1)}\right.\\ &\left.+\frac{(\xi-1)^k(1+\xi)^{k-2}}{2}+\frac{k^2(\xi-1)^{k-1}(1+\xi)^{k-2}}{(k-1)^2}\right]\\ =& \frac{2k-1}{2^{k-1}(k-1)!}\frac{d^{k-2}}{d\xi^{k-2}}\left[(\xi-1)^{k-1}(1+\xi)^{k-2}\left(\xi+\frac{k+1}{k-1}\right)\right].\end{aligned}$$

Let $f_k(\xi) = (\xi-1)^{k-1}(1+\xi)^{k-2}\left(\xi+\frac{k+1}{k-1}\right)$, which is a polynomial of degree $2k-2$. We note that the function $f_k(\xi)$ has $2k-2$ roots: the simple root $-\frac{k+1}{k-1}$, the root -1 (with multiplicity $k-2$), and the root 1 (with multiplicity $k-1$).

- By Rolle's Theorem, $f_k'(\xi)$ has $2k-3$ roots: one simple root $\xi_{1,1} \in (-\frac{k+1}{k-1}, -1)$, the root -1 (with multiplicity $k-3$), one simple root $\xi_{1,2} \in (-1,1)$, and the root 1 (with multiplicity $k-2$).
- Similarly, by Rolle's Theorem, $f_k''(\xi)$ has $2k-4$ roots: one simple root $\xi_{2,1} \in (-\xi_{1,1}, -1)$, the root -1 (with multiplicity $k-4$), one simple root $\xi_{2,2} \in (-1, \xi_{1,2})$, one simple root $\xi_{2,3} \in (\xi_{1,2}, 1)$, and the root 1 (with multiplicity $k-3$).
- Using an induction argument and Rolle's Theorem, we can show that the polynomial $\frac{d^{k-3}f_k}{d\xi^{k-3}}$ of degree $k+1$ has $k+1$ roots: one simple root < -1, the simple root -1, $k-3$ simple roots in $(-1,1)$, and the root 1 (with multiplicity two).
- Finally, Rolle's Theorem can be used to show that the polynomial $\frac{d^{k-2}f_k}{d\xi^{k-2}}$ of degree k has k roots: one root less than -1, $k-2$ distinct zeros in $(-1,1)$, and the simple root 1.

Since $\tilde{B}_k(\xi)$ is proportional to $\frac{d^{k-2}f_k}{d\xi^{k-2}}$, we conclude that $\tilde{B}_k(\xi)$ has k roots: one root less than -1, $k-2$ distinct zeros in $(-1,1)$, and the simple root 1.

Finally, we show (26). Since $\hat{B}_k(\xi)$ is a polynomial of degree k and has k distinct real roots $b_0 < b_1 < \cdots < b_{k-1} = 1$, we can factor it as $\hat{B}_k(\xi) = c_k \prod_{j=0}^{k-1}(\xi - b_j)$, where c_k is the coefficient of the term ξ^k. Since

$$\hat{B}_k(\xi) = \hat{L}_k(\xi) - \hat{L}_{k-1}(\xi) + \frac{k^2}{(k-1)^2}\left(\hat{L}_{k-1}(\xi) - \hat{L}_{k-2}(\xi)\right), \quad -1 \le \xi \le 1,$$

we deduce that c_k is the coefficient of the term ξ^k in $\hat{L}_k(\xi)$. Using (20) with $\alpha = \beta = 0$ and the fact that $\Gamma(k+1) = k!$, the coefficient of the term ξ^k in $\hat{L}_k(\xi)$ is $c_k = \frac{\Gamma(2k+1)}{2^k k!\Gamma(k+1)} = \frac{(2k)!}{2^k(k!)^2}$. Thus, we have $\hat{B}_k(\xi) = \frac{(2k)!}{2^k(k!)^2}\prod_{j=0}^{k-1}(\xi - b_j)$. This completes the proof of the lemma. □

3.3. Shifted Baccouch polynomials. Mapping the physical element I_i into the reference element $[-1,1]$ by the standard affine mapping (21), we get the k-degree

shifted Baccouch polynomial $B_{k,i}(x)$ on I_i

$$B_{k,i}(x) = \hat{B}_k\left(\frac{2x - x_i - x_{i-1}}{h_i}\right), \quad x \in I_i. \tag{27}$$

Throughout this paper, the roots of the k-degree polynomial $\hat{B}_k(\xi)$ are denoted by $b_j,\ j = 0, 1, \ldots, k-1$ and the roots of the k-degree polynomial $B_{k,i}(x)$ for $x \in I_i$ are defined by

$$x_{i,j} = \frac{h_i}{2} b_j + \frac{x_i + x_{i-1}}{2}, \quad j = 0, 1, \ldots, k-1. \tag{28}$$

Using (26) and (27), we get

$$\begin{aligned} B_{k,i}(x) &= \frac{(2k)!}{2^k (k!)^2} \prod_{j=0}^{k-1} \left(\frac{2x - x_i - x_{i-1}}{h_i} - \frac{2x_{i,j} - x_i - x_{i-1}}{h_i}\right) \\ &= \frac{(2k)!}{(k!)^2 h_i^k} \prod_{j=0}^{k-1} (x - x_{i,j}), \quad x \in I_i. \end{aligned} \tag{29}$$

Consequently, the $(p+1)$-degree shifted Baccouch polynomial $B_{p+1,i}(x)$ on I_i can be written as

$$B_{p+1,i}(x) = \frac{(2p+2)!}{((p+1)!)^2 h_i^{p+1}} \prod_{j=0}^{p} (x - x_{i,j}), \quad x \in I_i. \tag{30}$$

Next, we state some properties of $B_{p+1,i}$ which will be needed in our *a posteriori* error analysis.

Lemma 3.2. *The $(p+1)$-degree shifted Baccouch polynomial $B_{p+1,i}(x)$, $x \in I_i$ satisfies the following properties*

$$\int_{I_i} B_{p+1,i}^2(x)\, dx = \sigma_p h_i, \tag{31a}$$

$$\int_{I_i} B''_{p+1,i}(x) B_{p+1,i}(x)\, dx = -\frac{4(p+1)^2(2p+1)}{p^2 h_i} = \frac{\lambda_p}{h_i}, \tag{31b}$$

where $\sigma_p = \frac{1}{2p+3} + \frac{(2p+1)^2}{p^4}\frac{1}{2p+1} + \frac{(p+1)^4}{p^4}\frac{1}{2p-1}$ and $\lambda_p = -\frac{4(p+1)^2(2p+1)}{p^2}$ are constants independent of h.

Proof. Using the orthogonality relation (19), we have

$$\begin{aligned} \int_{I_i} B_{p+1,i}^2(x)\, dx &= \frac{h_i}{2} \int_{-1}^{1} \hat{B}_{p+1}^2(\xi)\, d\xi \\ &= \frac{h_i}{2} \int_{-1}^{1} \left(\hat{L}_{p+1}(\xi) + \frac{2p+1}{p^2}\hat{L}_p(\xi) - \frac{(p+1)^2}{p^2}\hat{L}_{p-1}(\xi)\right)^2 d\xi \\ &= \frac{h_i}{2} \int_{-1}^{1} \left(\hat{L}_{p+1}^2(\xi) + \frac{(2p+1)^2}{p^4}\hat{L}_p^2(\xi) + \frac{(p+1)^4}{p^4}\hat{L}_{p-1}^2(\xi)\right) d\xi \\ &= \left(\frac{1}{2p+3} + \frac{(2p+1)^2}{p^4}\frac{1}{2p+1} + \frac{(p+1)^4}{p^4}\frac{1}{2p-1}\right) h_i = \sigma_p h_i, \end{aligned}$$

where $\sigma_p = \frac{1}{2p+3} + \frac{(2p+1)^2}{p^4}\frac{1}{2p+1} + \frac{(p+1)^4}{p^4}\frac{1}{2p-1}$ is a constant independent of h. Furthermore, we have

$$\begin{aligned}\int_{I_i} B''_{p+1,i}(x)B_{p+1,i}(x)\,dx =& \frac{2}{h_i}\int_{-1}^{1} \hat{B}''_{p+1}(\xi)\hat{B}_{p+1}(\xi)\,d\xi \\ =& -\frac{2(p+1)^2}{p^2 h_i}\int_{-1}^{1} \hat{L}''_{p+1}(\xi)\hat{L}_{p-1}(\xi)\,d\xi.\end{aligned}$$

Integrating by parts twice, we get

$$\int_{I_i} B''_{p+1,i}(x)B_{p+1,i}(x)\,dx = -\frac{4(p+1)^2(2p+1)}{p^2 h_i} = \frac{\lambda_p}{h_i},$$

where $\lambda_p = -\frac{4(p+1)^2(2p+1)}{p^2}$ is a constant independent of h. □

Theorem 3.1. *Suppose that $b_1 < b_2 < \ldots < b_p = 1$ are the roots of $\hat{B}_{p+1}(\xi)$ in $(-1, 1]$. Then there exists a unique polynomial $\mathcal{I}_h u$ of degree at most p such that $\mathcal{I}_h(b_k) = u(b_k),\ k = 1, 2, \ldots, p$ and $(\mathcal{I}_h)'(-1) = u'(-1)$.*

Proof. We prove the existence as follows. Let $S_{p-1}(\xi)$ be the Lagrange interpolating polynomial of degree at most $p-1$ that interpolates $u(\xi)$ at roots $b_1, b_2, \ldots, b_p$ *i.e.*,

$$S_{p-1}(\xi) = \sum_{k=1}^{p} u(b_k) \prod_{j=1,\ j\neq k}^{p} \frac{\xi - b_j}{b_k - b_j}.$$

Let us now construct from $S_{p-1}(\xi)$ a new polynomial, $\mathcal{I}_h(\xi)$, in the following way:

$$\mathcal{I}_h u(\xi) = S_{p-1}(\xi) + \alpha \prod_{j=1}^{p}(\xi - b_j),$$

where α is a constant to be determined. By construction the degree of $\mathcal{I}_h(\xi)$ is at most p. In addition, we have $\mathcal{I}_h(b_k) = u(b_k),\ k = 1, 2, \ldots, p$. All that remains is to determine the constant α in such a way that the last interpolation condition, $(\mathcal{I}_h)'(-1) = u'(-1)$, is satisfied, *i.e.*,

$$u'(-1) = S'_{p-1}(-1) + \alpha \sum_{k=1}^{p} \prod_{j=1, j\neq k}^{p} (-1 - b_j).$$

This condition defines α as

$$\alpha = \frac{u'(-1) - S'_{p-1}(-1)}{\sum_{k=1}^{p} \prod_{j=1, j\neq k}^{p} (-1 - b_j)}.$$

This shows the existence.

To show the uniqueness, we assume there are two polynomials $P_1(\xi)$ and $P_2(\xi)$ of degree $\leq p$ such that $P_s(b_k) = u(b_k)$ for $k = 1, 2, \ldots, p$ and $P'_s(-1) = u'(-1)$ with $s = 1, 2$. We consider the difference $P(\xi) = P_1(\xi) - P_2(\xi)$. Since $P(b_k) = 0$, $k = 1, 2, \ldots, p$, $P(\xi)$ has at least p roots. Since $P(\xi)$ is a polynomial of degree $\leq p$ with p distinct roots, then it can be written as $P(\xi) = \beta \prod_{j=1}^{p} (\xi - b_j)$, where β is a constant. Furthermore, using the fact that $P'(-1) = 0$, we obtain $\beta \sum_{k=1}^{p} \prod_{j=1, j\neq k}^{p} (-1 - b_j) = 0$, which gives $\beta = 0$. Thus, $P(\xi) = 0$. Therefore the interpolating polynomial must be unique. □

3.4. Interpolating polynomials. Here, we define two interpolation operators Π_h and $\hat{\Pi}_h$. The operator Π_h is defined as follows: For any function $u = u(x)$, $\Pi_h u|_{I_i} \in \mathbb{P}^p(I_i)$ and interpolates u at the roots $x_{i,j},\ j = 0, 1, \ldots, p$, of the $(p+1)$-degree polynomial $B_{p+1,i}(x)$ on I_i *i.e.*, at the nodes $x_{i,j} = \frac{x_i - x_{i-1}}{2} b_j + \frac{x_i + x_{i-1}}{2}$, $j = 0, 1, \ldots, p$, where b_j are the roots of $\hat{B}_{p+1}(\xi)$ on $[-1, 1]$.

The operator $\hat{\Pi}_h$ is such that $\hat{\Pi}_h u|_{I_i} \in \mathbb{P}^{p+1}(I_i)$ and is defined as follows: $\hat{\Pi}_h u|_{I_i}$ interpolates u at $x_{i,j},\ j = 0, 1, \ldots, p$, and at an additional point $\bar{x}_i$ in I_i with $\bar{x}_i \neq x_{i,j},\ i = 0, 1, \ldots, p$. For simplicity we choose $\bar{x}_i = x_{i-1}$.

Remark 3.1. The operator $\hat{\Pi}_h$ is needed for technical reasons in the proof of the error estimates. We would like to mention that the interpolating polynomial $\hat{\Pi}_h u$ depends on the additional point $\bar{x}_i$. We note that we can easily verify the following

$$\hat{\Pi}_h u = \Pi_h u + c_{p+1} B_{p+1,i}(x). \tag{33}$$

Using (33) and the fact that $\hat{\Pi}_h u(\bar{x}_i) = u(\bar{x}_i)$, we find $c_{p+1} = \frac{u(\bar{x}_i) - \Pi_h u(\bar{x}_i)}{B_{p+1,i}(\bar{x}_i)}$.

In the next lemma, we prove some properties of $B_{p+1,i}(x)$ which will be needed in our *a posteriori* error analysis. In particular, we show that the interpolation error can be divided into dominant and less dominant parts.

Lemma 3.3. *Let $P_h^- u$ be the projection defined in (4) and $\Pi_h u$ be the interpolating polynomial that interpolated u at $x_{i,j},\ j = 0, 1, \ldots, p,$. Then*

$$P_h^- L_{p+1,i}(x) = \Pi_h L_{p+1,i}(x) = L_{p,i}(x) - \frac{(p+1)^2}{p^2} R_{p,i}(x). \tag{34}$$

Consequently, we have

$$\Pi_h v = P_h^- v, \quad \forall\ v \in \mathbb{P}^{p+1}(I_i). \tag{35}$$

Moreover, if $u \in H^{p+2}(I_i)$ then the interpolation error $u - \Pi_h u$ can be split as:

$$u - \Pi_h u = \phi_i + \gamma_i, \quad \phi_i = a_i B_{p+1,i}(x), \quad \gamma_i = u - \hat{\Pi}_h u, \quad \text{on } I_i, \tag{36}$$

where a_i is the coefficient of $B_{p+1,i}$ in the $(p+1)$-degree interpolating polynomial $\hat{\Pi}_h u$ and

$$\|\phi_i\|_{k,I_i} \leq C h_i^{p+1-k} \|u\|_{p+1,I_i}, \quad 0 \leq k \leq p, \tag{37a}$$

$$\|\gamma_i\|_{k,I_i} \leq C h_i^{p+2-k} \|u\|_{p+2,I_i}, \quad 0 \leq k \leq p+1. \tag{37b}$$

Finally, we have the following superconvergence result

$$\left\|\Pi_h u - P_h^- u\right\|_{0,I_i} \leq C h_i^{p+2} \|u\|_{p+2,I_i}. \tag{38}$$

Proof. First we show (34). Writing $P_h^- L_{p+1,i}(x) = \sum_{j=0}^{p} c_j L_{j,i}(x) \in \mathbb{P}^p(I_i)$ and using the properties in (4), we get

$$\sum_{j=0}^{p} c_j \int_{I_i} L_{j,i}(x) v\, dx = \int_{I_i} L_{p+1,i} v\, dx,\ \forall\ v \in \mathbb{P}^{p-2}(I_i), \tag{39}$$

$$\sum_{j=0}^{p} c_j L'_{j,i}(x_{i-1}) = L'_{p+1,i}(x_{i-1}), \quad \sum_{j=0}^{p} c_j L_{j,i}(x_i) = L_{p+1,i}(x_i). \tag{40}$$

Taking $v = L_{k,i}(x)$, $k = 0, 1, \ldots, p-2$ in (39), we get $c_k = 0$ for $k = 0, 1, \ldots, p-2$. Thus, $P_h^- L_{p+1,i}(x) = c_{p-1} L_{p-1,i}(x) + c_p L_{p,i}(x)$. Using $L_{j,i}(x_i) = 1$ and

$L'_{j,i}(x_{i-1}) = (-1)^{j+1}\frac{j(j+1)}{h_i}$, the two conditions in (40) give

$$(-1)^p\frac{(p-1)p}{h_i}c_{p-1} + (-1)^{p+1}\frac{p(p+1)}{h_i}c_p = (-1)^{p+2}\frac{(p+1)(p+2)}{h_i}, \quad c_{p-1}+c_p = 1,$$

which simplifies

$$(p-1)pc_{p-1} - p(p+1)c_p = (p+1)(p+2), \quad c_{p-1}+c_p = 1.$$

Solving the system for c_{p-1} and c_p, we obtain

$$c_{p-1} = \frac{(p+1)^2}{p^2}, \quad c_p = -\frac{2p+1}{p^2}.$$

Thus,

$$\begin{aligned} P_h^- L_{p+1,i}(x) =& \frac{(p+1)^2}{p^2}L_{p-1,i}(x) - \frac{2p+1}{p^2}L_{p,i}(x) \\ =& L_{p,i}(x) - \frac{(p+1)^2}{p^2}\left(L_{p,i}(x) - L_{p-1,i}(x)\right) \\ =& L_{p,i}(x) - \frac{(p+1)^2}{p^2}R_{p,i}(x). \end{aligned}$$

Using the standard interpolation error formula [8] and (30), there exists $y \in I_i$ such that the interpolation error $L_{p+1,i} - \Pi_h(L_{p+1,i})$ is

$$\begin{aligned} L_{p+1,i} - \Pi_h(L_{p+1,i}) =& \frac{L_{p+1,i}^{(p+1)}(y)}{(p+1)!}\prod_{j=0}^{p}(x - x_{i,j}) \\ =& \frac{(2p+2)!}{((p+1)!)^2 h_i^{p+1}}\prod_{j=0}^{p}(x - x_{i,j}) = B_{p+1,i}(x), \end{aligned}$$

since $L_{p+1,i}^{(p+1)}(y) = \frac{(2p+2)!}{(p+1)!h_i^{p+1}}$. Consequently, we have $\Pi_h(L_{p+1,i}) = L_{p+1,i}(x) - B_{p+1,i}(x)$. Since $B_{p+1,i}(x) = L_{p+1,i}(x) - L_{p,i}(x) + \frac{(p+1)^2}{p^2}R_{p,i}(x)$, we obtain

$$\begin{aligned} \Pi_h(L_{p+1,i}) =& L_{p+1,i}(x) - L_{p+1,i}(x) + L_{p,i}(x) - \frac{(p+1)^2}{p^2}R_{p,i}(x) \\ =& L_{p,i}(x) - \frac{(p+1)^2}{p^2}R_{p,i}(x). \end{aligned}$$

This completes the proof of (34).

Next, we show (35). Let $v \in \mathbb{P}^{p+1}(I_i)$. Then v can be split as $v(x) = v_1(x) + d_i L_{p+1,i}(x)$, where $v_1 \in \mathbb{P}^p(I_i)$ and d_i is a constant. Applying the operators Π_h and P_h^- and using the fact that $\Pi_h v_1 = P_h^- v_1 = v_1,\ \forall\ v_1 \in \mathbb{P}^p(I_i)$ yields

$$\Pi_h v = v_1 + d_i\Pi_h(L_{p+1,i}), \quad P_h^- v = v_1 + d_i P_h^-(L_{p+1,i}).$$

Thus, we have

$$v - \Pi_h v = d_i\left(L_{p+1,i} - \Pi_h(L_{p+1,i})\right), \quad v - P_h^- v = d_i\left(L_{p+1,i} - P_h^-(L_{p+1,i})\right). \tag{41}$$

Using (34), we get

$$v - \Pi_h v = d_i B_{p+1,i}(x) = v - P_h^- v. \tag{42}$$

Thus, we establish that

$$\Pi_h v = P_h^- v, \quad \forall\ v \in \mathbb{P}^{p+1}(I_i).$$

Next, we prove (36). Adding and subtracting $V = \hat{\Pi}_h u = \sum_{k=0}^{p} a_k L_{k,i} + a_i L_{p+1,i} \in \mathbb{P}^{p+1}(I_i)$, we split the interpolation error as

$$u - \Pi_h u = (u - V) + (V - \Pi_h u) = \phi_i + \gamma_i,\ \phi_i = V - \Pi_h u,\ \gamma_i = u - V = u - \hat{\Pi}_h u.$$

We note that, by (33), $\Pi_h u = \Pi_h(\hat{\Pi}_h u) = \Pi_h V$. Thus, by (34), we get

$$\begin{aligned}\phi_i = V - \Pi_h V &= \sum_{k=0}^{p} a_k L_{k,i} + a_i L_{p+1,i} - \Pi_h \left(\sum_{k=0}^{p} a_k L_{k,i} + a_i L_{p+1,i} \right) \\ &= a_i \left(L_{p+1,i} - \Pi_h(L_{p+1,i}) \right) = a_i B_{p+1,i}.\end{aligned}$$

Multiplying $\hat{\Pi}_h u = \sum_{k=0}^{p} a_k L_{k,i} + a_i L_{p+1,i}$ by $L_{p+1,i}$, integrating over I_i, and using the orthogonality relation (19), we obtain

$$\int_{I_i} L_{p+1,i} \hat{\Pi}_h u \, dx = \sum_{k=0}^{p} a_k \int_{I_i} L_{p+1,i} L_{k,i} dx + a_i \int_{I_i} L_{p+1,i} L_{p+1,i} dx = \frac{h_i}{2p+3} a_i,$$

which gives $a_i = \frac{2p+3}{h_i} \int_{I_i} L_{p+1,i} \hat{\Pi}_h u \, dx$. Thus, we completed the proof of (36).

Next, we will prove (37). By the standard interpolation error estimates we have

$$\|\phi_i\|_{k,I_i} \leq C_1 h_i^{p+1-k} \|V\|_{p+1,I_i}, \quad \|\gamma_i\|_{k,I_i} \leq C_2 h_i^{p+2-k} \|u\|_{p+2,I_i}. \tag{43}$$

Finally, we find a bound of $\|V\|_{p+1,I_i}$ by adding and subtracting u and applying the triangle inequality as

$$\begin{aligned}\|V\|_{p+1,I_i} \leq \|V - u\|_{p+1,I_i} + \|u\|_{p+1,I_i} &= \left\| \hat{\Pi}_h u - u \right\|_{p+1,I_i} + \|u\|_{p+1,I_i} \\ &\leq (C h_i + 1) \|u\|_{p+1,I_i} \leq C \|u\|_{p+1,I_i},\end{aligned}$$

which complete the proofs of (37).

In order to prove (38) we note that $\hat{\Pi}_h u \in \mathbb{P}^{p+1}(I_i)$, thus by (35) and (33), we have

$$P_h^-(\hat{\Pi}_h u) = \Pi_h(\hat{\Pi}_h u) = \Pi_h u, \tag{44}$$

and by the standard interpolation error we have

$$\left\| u - \hat{\Pi}_h u \right\|_{0,I_i} \leq C_1 h_i^{p+2} \|u\|_{p+2,I_i}. \tag{45}$$

Applying P_h^- to $u = u - \hat{\Pi}_h u + \hat{\Pi}_h u$ and using (44), we obtain

$$P_h^- u = P_h^-(u - \hat{\Pi}_h u) + P_h^-(\hat{\Pi}_h u) = P_h^-(u - \hat{\Pi}_h u) + \Pi_h u,$$

which, in turn, yields

$$P_h^- u - \Pi_h u = P_h^-(u - \hat{\Pi}_h u). \tag{46}$$

Now, we show that $\left\| P_h^- v \right\|_{0,I_i} \leq C_2 \|v\|_{0,I_i}$ by writing

$$\begin{aligned}\left\| P_h^- v \right\|_{0,I_i} = \left\| P_h^- v - v + v \right\|_{0,I_i} &\leq \left\| P_h^- v - v \right\|_{0,I_i} + \|v\|_{0,I_i} \\ &\leq C h_i^{p+1} \|v\|_{p+1,I_i} + \|v\|_{0,I_i} \leq C_2 \|v\|_{0,I_i}.\end{aligned} \tag{47}$$

Taking the L^2 norm of (46) and applying the estimate (47) with $v = u - \hat{\Pi}_h u$, we obtain

$$\left\| P_h^- u - \Pi_h u \right\|_{0,I_i} = \left\| P_h^-(u - \hat{\Pi}_h u) \right\|_{0,I_i} \leq C_2 \left\| u - \hat{\Pi}_h u \right\|_{0,I_i}. \tag{48}$$

Combining (48) and the standard interpolation estimates (45) we establish (38). □

Now, we are ready to state and prove the main global superconvergence result: the UWDG solution is $\mathcal{O}(h^{p+2})$ super close to $\Pi_h u$.

Theorem 3.2. *Under the assumptions of Theorem 2.1, there exists a positive constant C independent of h such that*

$$\|u_h - \Pi_h u\| \leq Ch^{p+2}. \tag{49}$$

Moreover, the true error can be divided into a dominant part and a less dominant part as

$$e_u(x) = \alpha_i B_{p+1,i}(x) + \omega_i(x), \quad x \in I_i, \tag{50a}$$

where

$$\omega_i = \gamma_i + \Pi_h u - u_h, \tag{50b}$$

and

$$\sum_{i=1}^{N} \left\| \frac{d^k \omega_i}{dx^k} \right\|_{0,I_i}^2 \leq Ch^{2(p+2-k)}, \qquad k = 0, 1, 2. \tag{50c}$$

Finally,

$$\|e_u'\| = \left(\sum_{i=1}^{N} \|e_u'\|_{0,I_i}^2 \right)^{1/2} \leq Ch^p, \quad \|e_u\|_1 \leq Ch^p. \tag{51}$$

Proof. Adding and subtracting $P_h^- u$ to $u_h - \Pi_h u$, we write

$$u_h - \Pi_h u = (u_h - P_h^- u) + (P_h^- u - \Pi_h u) = -\xi_u + P_h^- u - \Pi_h u.$$

Taking the L^2-norm and applying the triangle inequality, we obtain

$$\|u_h - \Pi_h u\| \leq \|\xi_u\| + \left\|P_h^- u - \Pi_h u\right\|.$$

Using the estimates (13) and (38), we establish (49).

Next, we add and subtract $\Pi_h u$ to e_u, we have

$$e_u = u - \Pi_h u + \Pi_h u - u_h. \tag{52}$$

Furthermore, one can split the interpolation errors $u - \Pi_h u$ on I_i as in (36) to obtain

$$e_u = \phi_i + \gamma_i + \Pi_h u - u_h = \phi_i + \omega_i, \quad \text{where} \quad \omega_i = \gamma_i + \Pi_h u - u_h. \tag{53}$$

Next, we will prove (50c). Using the Cauchy-Schwarz inequality and the inequality $2|ab| \leq a^2 + b^2$, we write for $k = 0, 1, 2$,

$$\begin{aligned}
\left\| \frac{d^k \omega_i}{dx^k} \right\|_{0,I_i}^2 &= \int_{I_i} \left(\frac{d^k \gamma_i}{dx^k} + \frac{d^k (\Pi_h u - u_h)}{dx^k} \right)^2 dx \\
&= \left\| \frac{d^k \gamma_i}{dx^k} \right\|_{0,I_i}^2 + 2 \int_{I_i} \frac{d^k \gamma_i}{dx^k} \frac{d^k (\Pi_h u - u_h)}{dx^k} \, dx + \left\| \frac{d^k (\Pi_h u - u_h)}{dx^k} \right\|_{0,I_i}^2 \\
&\leq 2 \left(\left\| \frac{d^k \gamma_i}{dx^k} \right\|_{0,I_i}^2 + \left\| \frac{d^k (\Pi_h u - u_h)}{dx^k} \right\|_{0,I_i}^2 \right).
\end{aligned}$$

Using the inverse inequality $\left\| \frac{d^k(\Pi_h u - u_h)}{dx^k} \right\|_{0,I_i} \leq C\ h^{-k} \left\| \Pi_h u - u_h \right\|_{0,I_i}$, we obtain the estimate

$$\left\| \frac{d^k \omega_i}{dx^k} \right\|_{0,I_i}^2 \leq 2 \left(\left\| \frac{d^k \gamma_i}{dx^k} \right\|_{0,I_i}^2 + h^{-2k} \left\| \frac{d^k (\Pi_h u - u_h)}{dx^k} \right\|_{0,I_i}^2 \right).$$

Summing over all elements and applying (37b) and (49) yields

$$\left\| \frac{d^k \omega_i}{dx^k} \right\|_{0,I_i}^2 \leq 2 \left(C_1 h^{2(p+2-k)} + h^{-2k} C_2 h^{2(p+2)} \right) \leq C h^{2(p+2-k)},$$

which gives the estimate (50c).

In order to show (51), we note that

$$\|e_u\|_{1,\Omega}^2 = \|e_u\|^2 + \sum_{i=1}^{N} \|e_u'\|_{0,I_i}^2 . \tag{54}$$

Differentiating (53) with respect to x, taking the L^2-norm, and applying the Cauchy-Schwarz inequality and the inequality $|ab| \leq \frac{1}{2}(a^2 + b^2)$, we get

$$\|e_u'\|_{0,I_i}^2 = (\phi_i' + \omega_i', \phi_i' + \omega_i')_{I_i} \leq 2 \left(\|\phi_i'\|_{0,I_i}^2 + \|\omega_i'\|_{0,I_i}^2 \right).$$

Summing over all elements and applying (37a) and (50c), we obtain

$$\sum_{i=1}^{N} \|e_u'\|_{0,I_i}^2 \leq C h^{2p}. \tag{55}$$

Finally, substituting (11) and (55) into (54) establishes (51). □

4. *A posteriori* error estimation

In this section, we present a technique to compute asymptotically correct *a posteriori* estimates of the UWDG errors for the nonlinear BVP (1). These estimates are computed by solving a local problem with no boundary condition on each element. We further prove that the UWDG discretization error estimates converge to the true spatial errors in the L^2-norm as $h \to 0$. Next, we present the weak finite element formulation to compute *a posteriori* error estimate for the nonlinear BVP (1).

Multiplying (1) by arbitrary smooth function v and integrating over an arbitrary element I_i, we get

$$\int_{I_i} u'' v \, dx = \int_{I_i} v f(x,u) \, dx. \tag{56}$$

Replacing u by $u_h + e_u$, we obtain

$$\int_{I_i} e_u'' v \, dx = \int_{I_i} v \left(f(x, u_h + e_u) - u_h'' \right) dx. \tag{57}$$

Substituting (50a), *i.e.*, $e_u = \alpha_i B_{p+1,i}(x) + \omega_i$, into the left-hand side of (57) and choosing $v = B_{p+1,i}$ yields

$$\alpha_i \int_{I_i} B_{p+1,i}'' B_{p+1,i} dx = \int_{I_i} B_{p+1,i} \left(f(x, u_h + e_u) - u_h'' - \omega_i'' \right) dx. \tag{58}$$

Solving for α_i and using (31b), we obtain

$$\alpha_i = \frac{h_i}{\lambda_p} \int_{I_i} B_{p+1,i} \left(f(x, u_h + e_u) - u_h'' - \omega_i'' \right) dx. \tag{59}$$

Our error estimate procedure consists of approximating the true error on each element I_i by the leading term as

$$e_u(x) \approx E_u(x) = a_i B_{p+1,i}(x), \quad x \in I_i, \tag{60a}$$

where the coefficient of the leading term of the error, a_i, is obtained from the coefficient α_i defined in (59) by neglecting the unknown terms ω_i and e_u, *i.e.*,

$$a_i = \frac{h_i}{\lambda_p} \int_{I_i} B_{p+1,i} \left(f(x, u_h) - u_h'' \right) dx. \tag{60b}$$

We note that our error estimates are obtained by solving local problems with no boundary conditions.

An accepted efficiency measure of *a posteriori* error estimates is the effectivity index. In this paper, we use the global effectivity index

$$\Theta = \frac{\|E_u\|}{\|e_u\|},$$

and is used to appraise the accuracy of the error estimate. Ideally, the global effectivity index should stay close to one and should converge to one under mesh refinement; [6].

Remark 4.1. A standard measure of the quality of an estimator is the so-called effectivity index. A property that has been considered highly relevant to measure the potential quality of an estimator is the so-called asymptotic exactness. Roughly speaking, an estimator is asymptotically exact for a particular problem if its effectivity index converges to one when the meshsize approaches zero. For more details consult [6].

Next, we will show that the error estimate E_u converges to the exact error e_u in the L^2-norm as $h \to 0$. Furthermore, we will prove the convergence to unity of the global effectivity index Θ under mesh refinement.

The main results of this section are stated in the following theorem. In particular, we state and prove asymptotic results of our *a posteriori* error estimates.

Theorem 4.1. *Suppose that the assumptions of Theorem 2.1 are satisfied. If* $E_u = a_i B_{p+1,i}(x),\ x \in\ I_i$, *where* $a_i,\ i = 1, 2, \ldots, N$, *are given by (60b), then there exists a positive constant* C *independent of* h *such that*

$$\|e_u - E_u\| \leq C\ h^{p+2}, \tag{61}$$

$$\big|\, \|e_u\| - \|E_u\| \,\big| \leq C_1 h^{p+2}. \tag{62}$$

As a consequence, the UWDG method combined with the a posteriori error estimation procedure yields $\mathcal{O}(h^{p+2})$ *superconvergent solution i.e.*,

$$\|e_u - E_u\|^2 = \|u - (u_h + E_u)\|^2 = \sum_{i=1}^{N} \|u - (u_h + a_i B_{p+1,i})\|_{0,I_i}^2 \leq C\ h^{2p+4}. \tag{63}$$

Finally, if there exists a constant $C = C(u) > 0$ *independent of* h *such that*

$$\|e_u\| \geq C h^{p+1}, \tag{64}$$

then the global effectivity index in the L^2 norm, which is defined as $\Theta_u = \frac{\|E_u\|}{\|e_u\|}$, converges to unity at $\mathcal{O}(h)$ rate i.e.,

$$\Theta_u = 1 + \mathcal{O}(h). \tag{65}$$

Proof. First, we will prove (61). Since $e_u = \alpha_i B_{p+1,i} + \omega_i$ and $E_u = a_i B_{p+1,i}$ on I_i, we have

$$\|e_u - E_u\|^2_{0,I_i} = \|(\alpha_i - a_i)B_{p+1,i} + \omega_i\|^2_{0,I_i} \leq 2(\alpha_i - a_i)^2 \|B_{p+1,i}\|^2_{0,I_i} + 2\|\omega_i\|^2_{0,I_i},$$

where we used the inequality $(a+b)^2 \leq 2a^2 + 2b^2$. Summing over all elements and applying the estimate (50c) yields

$$\begin{aligned}\|e_u - E_u\|^2 = \sum_{i=1}^{N} \|e_u - E_u\|^2_{0,I_i} &\leq 2\sum_{i=1}^{N}(\alpha_i - a_i)^2 \|B_{p+1,i}\|^2_{0,I_i} + 2\sum_{i=1}^{N}\|\omega_i\|^2_{0,I_i} \\ &\leq 2\sum_{i=1}^{N}(\alpha_i - a_i)^2 \|B_{p+1,i}\|^2_{0,I_i} + 2C_1 h^{2p+4}. \end{aligned} \tag{66}$$

Next, we will estimate $\sum_{i=1}^{N}(\alpha_i - a_i)^2 \|B_{p+1,i}\|^2_{0,I_i}$. Subtracting (60b) from (59), we obtain

$$\alpha_i - a_i = \frac{h_i}{\lambda_p}\int_{I_i} B_{p+1,i}\left(f(x, u_h + e_u) - f(x, u_h) - \omega_i''\right) dx. \tag{67}$$

Thus,

$$|\alpha_i - a_i| \leq \frac{h_i}{\lambda_p}\int_{I_i} |B_{p+1,i}|\left(|f(x, u_h + e_u) - f(x, u_h)| + |\omega_i''|\right) dx. \tag{68}$$

Using the Lipschitz condition (9) and applying the Cauchy-Schwarz inequality yields

$$\begin{aligned}|\alpha_i - a_i| \leq& \frac{h_i}{\lambda_p}\int_{I_i} |B_{p+1,i}|\left(L|e_u| + |\omega_i''|\right) dx \\ \leq& \frac{h_i \|B_{p+1,i}\|_{0,I_i}}{\lambda_p}\left(L\|e_u\|_{0,I_i} + \|\omega_i''\|_{0,I_i}\right). \end{aligned} \tag{69}$$

Squaring both sides and applying the inequality $(a+b)^2 \leq 2(a^2+b^2)$, we obtain

$$(\alpha_i - a_i)^2 \leq \frac{2h_i^2 \|B_{p+1,i}\|^2_{0,I_i}}{\lambda_p^2}\left(L^2\|e_u\|^2_{0,I_i} + \|\omega_i''\|^2_{0,I_i}\right). \tag{70}$$

Multiplying by $\|B_{p+1,i}\|^2_{0,I_i}$ and using (31a), *i.e.*, $\|B_{p+1,i}\|^2_{0,I_i} = h_i\sigma_p$ yields

$$\begin{aligned}(\alpha_i - a_i)^2 \|B_{p+1,i}\|^2_{0,I_i} &\leq \frac{2h_i^2 \|B_{p+1,i}\|^4_{0,I_i}}{\lambda_p^2}\left(L^2\|e_u\|^2_{0,I_i} + \|\omega_i''\|^2_{0,I_i}\right) \\ &= \frac{2h_i^4\sigma_p^2}{\lambda_p^2}\left(L^2\|e_u\|^2_{0,I_i} + \|\omega_i''\|^2_{0,I_i}\right). \end{aligned}$$

Summing over all elements and using $h = \max_{1\leq i\leq N} h_i$, we arrive at

$$\sum_{i=1}^{N}(\alpha_i - a_i)^2 \|B_{p+1,i}\|^2_{0,I_i} \leq \frac{2h^4\sigma_p^2}{\lambda_p^2}\left(L^2\|e_u\|^2 + \sum_{i=1}^{N}\|\omega_i''\|^2_{0,I_i}\right).$$

Combining this estimate with (11) and (50c), we get

$$\sum_{i=1}^{N}(\alpha_i - a_i)^2 \left\|B_{p+1,i}\right\|_{0,I_i}^2 \leq \frac{2h^4\sigma_p^2}{\lambda_p^2}\left(L^2C_1h^{2p+2} + C_2h^{2p}\right) \leq C_3h^{2p+4}. \tag{71}$$

Now, combining (66) with (71) yields

$$\left\|e_u - E_u\right\|^2 \leq 2C_3h^{2p+4} + 2C_1h^{2p+4} \leq Ch^{2p+4},$$

which completes the proof of (61).

In order to prove (62), we use the reverse triangle inequality to have

$$\left|\, \left\|E_u\right\| - \left\|e_u\right\| \,\right| \leq \left\|E_u - e_u\right\|. \tag{72}$$

Combining (72) and (61) completes the proof of (62).

Using the relation $e_u = u - u_h$ and the estimate (61), we obtain

$$\sum_{i=1}^{N}\left\|u - (u_h + a_iB_{p+1,i})\right\|_{0,I_i}^2 = \left\|u - (u_h + E_u)\right\|^2 = \left\|e_u - E_u\right\|^2 \leq Ch^{2p+4}.$$

In order to prove (65), we divide the inequality in (72) by $\|e_u\|$ and we use the estimate (61) and the assumption (64) to obtain

$$\left|\frac{\|E_u\|}{\|e_u\|} - 1\right| \leq \frac{\|E_u - e_u\|}{\|e_u\|} \leq \frac{C_1h^{p+2}}{C_2h^{p+1}} \leq Ch.$$

Therefore, $\frac{\|E_u\|}{\|e_u\|} = 1 + \mathcal{O}(h)$, which completes the proof of (65). □

In the previous theorem, we proved that the global *a posteriori* error estimates converge to the true spatial errors at $\mathcal{O}(h^{p+2})$ rate. We further proved that the global effectivity index in the L^2-norm converges to unity at $\mathcal{O}(h)$ rate.

Remark 4.2. Since $e_u = u - u_h$, we have $e_u - E_u = u - (u_h + E_u)$. Using (61) to get $\|u - (u_h + E_u)\| = \|e_u - E_u\| \leq Ch^{p+2}$. Thus, the computable post-processed solution defined by $u_h^* = u_h + E_u$ converges to the exact solution u at $\mathcal{O}(h^{p+2})$ rate. This accuracy enhancement is simply achieved by adding the error estimate E_u to the approximate UWDG solution u_h only once at the end of the computation. We would like to point out that our error estimates are obtained by solving a local problem with no boundary conditions on each element. This leads to very efficient computations of the post-processed approximation $u_h + E_u$.

Remark 4.3. The performance of an error estimator is commonly measured by the effectivity index which is the ratio of the estimated error to the actual error. In particular, we say that the error estimator is asymptotically exact if the effectivity index approaches unity as the mesh size goes to zero. Thus, (65) indicated that our *a posteriori* error estimator is asymptotically exact. We note that E_u is a computable quantity since it only depends on the numerical solution u_h and the f. It provides an asymptotically exact *a posteriori* estimator on the actual error $\|e_u\|$. We would like to emphasize that our UWDG error estimate is computationally simple which make it useful in adaptive computations.

Remark 4.4. The assumption (64) implies that terms of order $\mathcal{O}(h^{p+1})$ are present in the error. If this were not the case, the error estimate E_u might not be such a good approximation of the error e_u. Even though the proof of (65) is valid under the assumption (64), our computational results given in the next section demonstrate that the global effectivity index in the L^2-norm converge to unity at

$\mathcal{O}(h)$ rate. Thus, the proposed error estimation technique is an excellent measure of the error. We note that the *a priori* estimate (11) is optimal in the sense that the exponent of h is the largest possible. In fact, one may show that provided that the $(p+1)$st-order derivatives of the exact solution u do not vanish identically over the domain ($u \notin V_h^p$), then an inverse estimate of the form (64) is valid for some positive constant C (see [3, 20, 21]), which depends on u, but not on h. Combining (11) with (64), we show that u_h approximates u to $\mathcal{O}(h^{p+1})$ in the L^2 norm.

5. Numerical examples

In this section, we provide several numerical examples to verify our theoretical findings. In our experiments, the system of nonlinear algebraic equations resulting from the UWDG scheme (3) is approximated using the Newton-Raphson method. The stopping criterion for Newton's iteration is taken 10^{-15}. In all examples, we will compute the L^2 errors $\|u_h - \Pi_h u\|$, $\|e_u - E_u\|$, and $|\|e_u\| - \|E_u\||$. In all numerical experiments, the numerical order of convergence is computed using the formula $-\frac{\ln(||e_u^{N_1}||/||e_u^{N_2}||)}{\ln(N_1/N_2)}$, where $e_u^{N_1}$ and $e_u^{N_2}$ denote the errors using N_1 and N_2 elements, respectively.

For easy visualization, we plot the L^2-errors in log scale. For each degree p, we fit, in a least-squares sense, the data sets with a linear polynomial function and then we compute the slope of the fitting line.

Example 5.1. In this example, we consider the following linear BVP

$$u'' = u - 2\sin(x), \quad x \in [0, 2\pi], \quad u(0) = 1, \quad u'(2\pi) = 1, \tag{73}$$

where the analytical solution is $u(x) = \sin(x)$. We note that $f(x, u) = u - 2\sin(x)$, which satisfies all conditions used in the theorems. We solve (73) using the UWDG scheme presented in Section 2. We uniformly discretize the spatial interval $[0, 2\pi]$ through vertices $x_i = ih$, $i = 0, 1, \ldots, N$, $h = 2\pi/N$. The L^2 errors $\|u_h - \Pi_h u\|$ are reported in left figure of Figure 1. These results indicate that the UWDG solution u_h is $\mathcal{O}(h^{p+2})$ super close to $\Pi_h u$. This is in full agreement with Theorem 3.2.

Next, we implement the proposed error estimation procedure presented in Section 4 to find the error estimator E_u on each element and the error $\|e_u - E_u\|$. In the left figure of Figure 2, we show the L^2-norm of the errors between e_u and E_u. These results indicate that $\|e_u - E_u\|$ is $\mathcal{O}(h^{p+2})$ in the L^2-norm for $p = 2, 3, 4, 5$. In the right figure of Figure 2, we show the convergence rates for the global errors $|\|e_u\| - \|E_u\||$. We observe that $|\|e_u\| - \|E_u\|| = \mathcal{O}(h^{p+2})$ as $h \to 0$. We conclude that our *a posteriori* error estimate E_u converges to the actual error e_u as $h \to 0$. These results are in full agreement with the theoretical estimate of Theorem 4.1. Thus, the above experiments show that the orders of convergence given in this paper are sharp.

We present the global effectivity indices Θ_u in Table 3. We see that Θ_u is near unity and converges to one under h-refinement. Finally, the errors $|\Theta_u - 1|$ and their orders of convergence shown in right figure of Figure 1 suggest that $|\Theta_u - 1|$ is $\mathcal{O}(h)$. Thus, the numerical convergence rate is the same as the theoretical rate derived in Theorem 4.1.

We repeat the previous example with all parameters kept unchanged except that we use the periodic boundary conditions *i.e.*, we consider

$$u'' = u - 2\sin(x), \quad x \in [0, 2\pi], \quad u(0) = u(2\pi), \quad u'(0) = u'(2\pi). \tag{74}$$

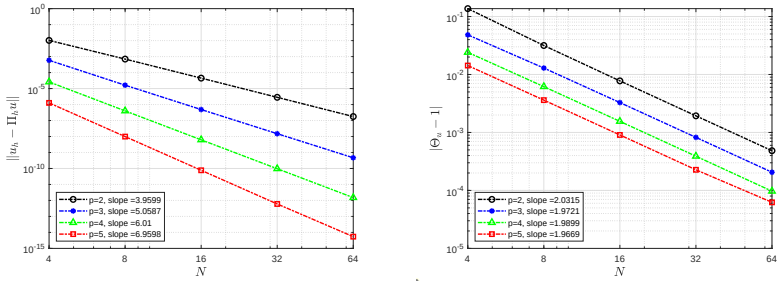

Figure 1: Convergence rates for $\|u_h - \Pi_h u\|$ (left) and $\|\Theta_u - 1\|$ (right) for the BVP (73) on uniform meshes having $N = 4$, 8, 16, 32, 64 elements using $p = 2$-5.

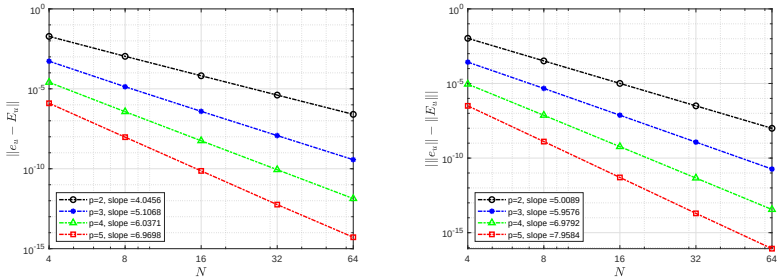

Figure 2: Convergence rates for $\|e_u - E_u\|$ (left) and $|\|e_u\| - \|E_u\||$ (right) for the BVP (73) on uniform meshes having $N = 4$, 8, 16, 32, 64 elements using $p = 2$-5.

TABLE 3. Global effectivity indices for Example 5.1 on uniform meshes having $N = 4$, 8, 16, 32, 64 elements using $p = 2 - 5$.

$p\backslash N$	$N = 4$	$N = 8$	$N = 16$	$N = 32$	$N = 64$
$p = 2$	1.1368	1.0316	1.0078	1.0019	1.0005
$p = 3$	1.0483	1.0129	1.0033	1.0008	1.0002
$p = 4$	1.0241	1.0062	1.0016	1.0004	1.0001
$p = 5$	1.0143	1.0036	1.0009	1.0002	1.0001

We use the uniform mesh with $N = 4$, 8, 16, 32, 64 elements and we find the UWDG solution $u_h \in V_h^p$ with $p = 2$, 3, 4, 5. The L^2 errors presented in the right figure of Figure 3 indicate that the UWDG solution u_h is $\mathcal{O}(h^{p+2})$ super close to $\Pi_h u$. This is in full agreement with the theory. In the left figure of Figure 4, we present the L^2-norm of the errors between e_u and E_u. These results indicate that $\|e_u - E_u\| = \mathcal{O}(h^{p+2})$. The results shown in the right figure of Figure 4 indicate that $|\|e_u\| - \|E_u\|| = \mathcal{O}(h^{p+2})$ as $h \to 0$. Once again we observe that our *a posteriori* error estimate E_u converges to the actual error e_u as $h \to 0$. These results are in full agreement with the theoretical estimate of Theorem 4.1. Next, we present the global effectivity indices Θ_u in Table 4. We observe that Θ_u is near unity and converges to one under h-refinement. Finally, the errors $|\Theta_u - 1|$ and their orders of convergence shown in the right figure of Figure 3 suggest that $|\Theta_u - 1|$ is $\mathcal{O}(h)$. Thus, the numerical convergence rate is the same as the theoretical rate derived in Theorem 4.1.

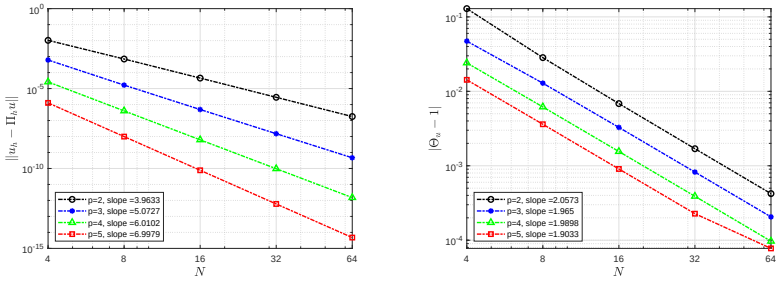

Figure 3: Convergence rates for $\|u_h - \Pi_h u\|$ (left) and $\|\Theta_u - 1\|$ (right) for the BVP (74) on uniform meshes having $N = 4$, 8, 16, 32, 64 elements using $p = 2$-5.

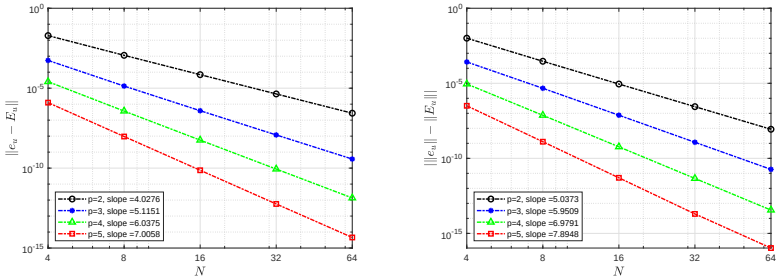

Figure 4: Convergence rates for $\|e_u - E_u\|$ (left) and $|\|e_u\| - \|E_u\||$ (right) for the BVP (74) on uniform meshes having $N = 4$, 8, 16, 32, 64 elements using $p = 2$-5.

TABLE 4. Global effectivity indices for the BVP (74) on uniform meshes having $N = 4$, 8, 16, 32, 64 elements using $p = 2 - 5$.

$p\backslash N$	$N = 4$	$N = 8$	$N = 16$	$N = 32$	$N = 64$
$p = 2$	1.1291	1.0284	1.0068	1.0017	1.0004
$p = 3$	1.0472	1.0129	1.0033	1.0008	1.0002
$p = 4$	1.0241	1.0062	1.0016	1.0004	1.0001
$p = 5$	1.0143	1.0036	1.0009	1.0002	1.0001

Example 5.2. In this example, we consider the following nonlinear BVP

$$u'' = \tan(u) - \cos(x) - \tan(\cos(x)), \quad x \in [0, 2\pi], \quad u(0) = 1, \quad u'(2\pi) = 0, \tag{75}$$

where the analytical solution is $u(x) = \cos(x)$. Here, $f(x, u) = \tan(u) - \cos(x) - \tan(\cos(x))$, which does not satisfy the assumptions in the theorems. We uniformly discretize the spatial interval $[0, 2\pi]$ through vertices $x_i = ih$, $i = 0, 1, \ldots, N$, $h = 2\pi/N$. The errors $\|u_h - \Pi_h u\|$, $\|e_u - E_u\|$, $|\|e_u\| - \|E_u\||$, and $|\Theta_u - 1|$ are shown in Figure 5 and Figure 6 for p= 2, 3,4 ,5. The rates of convergence obtained agree with the theoretical rates of convergence stated in Theorems 3.2 and 4.1, *i.e.*, our estimates are sharp. Finally, Table 5 displays the global effectivity index Θ. We can observe that the global effectivity indices stay close to unity and converge to unity under h-refinement.

We repeat the previous example with all parameters kept unchanged except that we use the periodic boundary conditions *i.e.*, we consider

$$u'' = \tan(u) - \cos(x) - \tan(\cos(x)), \quad x \in [0, 2\pi], \quad u(0) = u(2\pi), \quad u'(0) = u'(2\pi). \tag{76}$$

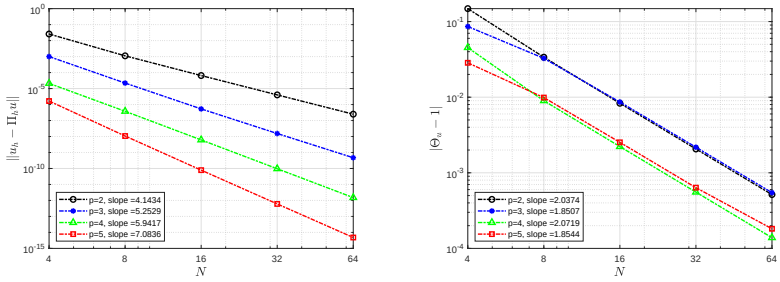

Figure 5: Convergence rates for $\|u_h - \Pi_h u\|$ (right) and $\|\Theta_u - 1\|$ (left) for the BVP (75) on uniform meshes having $N = 4$, 8, 16, 32, 64 elements using $p = 2$-5.

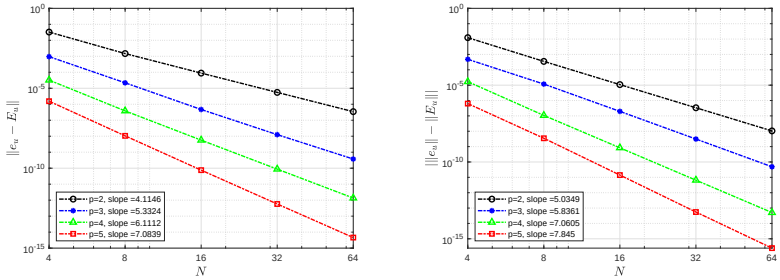

Figure 6: Convergence rates for $\|e_u - E_u\|$ (left) and $|\|e_u\| - \|E_u\||$ (right) for the BVP (75) on uniform meshes having $N = 4$, 8, 16, 32, 64 elements using $p = 2$-5.

TABLE 5. Global effectivity indices for Example 5.2 on uniform meshes having $N = 4$, 8, 16, 32, 64 elements using $p = 2 - 5$.

$p\backslash N$	$N = 4$	$N = 8$	$N = 16$	$N = 32$	$N = 64$
$p = 2$	1.1484	1.0338	1.0083	1.0021	1.0005
$p = 3$	1.0861	1.0327	1.0086	1.0022	1.0005
$p = 4$	1.0453	1.0090	1.0022	1.0006	1.0001
$p = 5$	1.0285	1.0099	1.0025	1.0006	1.0002

In Figures 7 and 8, we list the errors $\|u_h - \Pi_h u\|$, $\|e_u - E_u\|$, $|\|e_u\| - \|E_u\||$, and $|\Theta_u - 1|$ on logarithmic scales. We also show the numerical orders of convergence. We observe that $\|u_h - \Pi_h u\| = \mathcal{O}(h^{p+2})$, $\|e_u - E_u\| = \mathcal{O}(h^{p+2})$, $|\|e_u\| - \|E_u\|| = \mathcal{O}(h^{p+2})$, and $|\Theta_u - 1| = \mathcal{O}(h)$. The results showing in Table 6 indicate that the global effectivity index $\Theta \to 1$ under mesh refinement. Once again, the computed order of convergence matches with the theoretical order of convergence derived in Theorems 3.2 and 4.1.

Example 5.3. In this example, we consider the following BVP

$$u'' + e^{-u} = e^x + e^{-e^x}, \quad x \in [0, 3], \quad u(0) = 1, \quad u'(3) = e^3. \tag{77}$$

The exact solution is given by $u(x) = e^x$. In this example $f(x, u) = e^x + e^{-e^x} - e^{-u}$, which does not satisfy the Lipschitz condition (8). We implement the UWDG scheme using uniform mesh with $N = 5$, 10, 15, 20, 25, 30 elements and $p = 2$, 3, 4, 5. We present the errors $\|u_h - \Pi_h u\|$, $\|e_u - E_u\|$, $|\|e_u\| - \|E_u\||$, and $|\Theta_u - 1|$ in Figure 9 and Figure 10. Clearly, we observe $\|u_h - \Pi_h u\| = \mathcal{O}(h^{p+2})$,

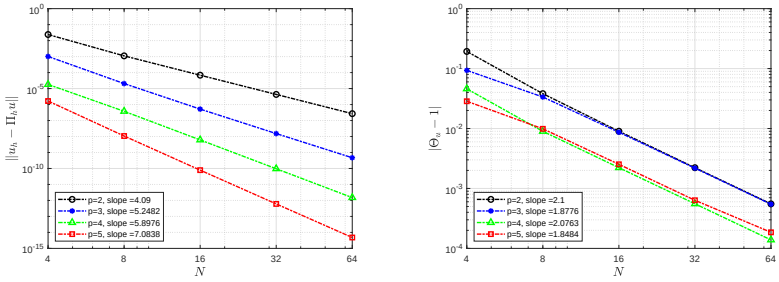

Figure 7: Convergence rates for $\|u_h - \Pi_h u\|$ (left) and $\|\Theta_u - 1\|$ (right) for the BVP (76) on uniform meshes having $N = 4$, 8, 16, 32, 64 elements using $p = 2$-5.

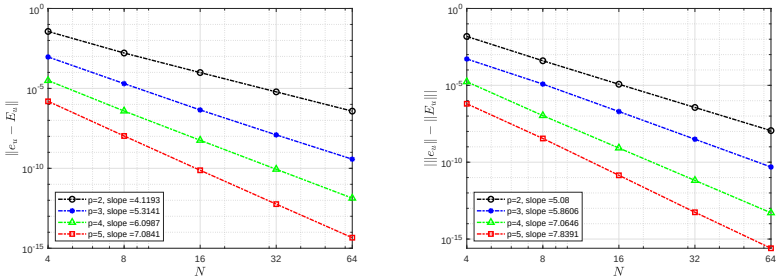

Figure 8: Convergence rates for $\|e_u - E_u\|$ (left) and $|\|e_u\| - \|E_u\||$ (right) for the BVP (76) on uniform meshes having $N = 4$, 8, 16, 32, 64 elements using $p = 2$-5.

TABLE 6. Global effectivity indices for the BVP (76) on uniform meshes having $N = 4$, 8, 16, 32, 64 elements using $p = 2 - 5$.

$p\backslash N$	$N = 4$	$N = 8$	$N = 16$	$N = 32$	$N = 64$
$p = 2$	1.1931	1.0381	1.0090	1.0022	1.0006
$p = 3$	1.0934	1.0335	1.0087	1.0022	1.0005
$p = 4$	1.0460	1.0090	1.0022	1.0006	1.0001
$p = 5$	1.0285	1.0099	1.0025	1.0006	1.0002

$\|e_u - E_u\| = \mathcal{O}(h^{p+2})$, $|\|e_u\| - \|E_u\|| = \mathcal{O}(h^{p+2})$, and $|\Theta_u - 1| = \mathcal{O}(h)$. The global effectivity indices Θ_u are shown in Table 7. We observe that Θ_u is near unity and converges to one under h-refinement. These results are in full agreement with our theoretical results.

TABLE 7. Global effectivity indices for Example 5.3 on uniform meshes having $N = 5$, 10, 15, 20, 25, 30 elements using $p = 2 - 5$.

$p\backslash N$	$N = 5$	$N = 10$	$N = 15$	$N = 20$	$N = 25$	$N = 30$
$p = 2$	1.0066	1.0033	1.0022	1.0017	1.0013	1.0011
$p = 3$	1.0044	1.0022	1.0015	1.0011	1.0009	1.0007
$p = 4$	1.0028	1.0014	1.0010	1.0007	1.0006	1.0005
$p = 5$	1.0019	1.0009	1.0006	1.0005	1.0004	1.0003

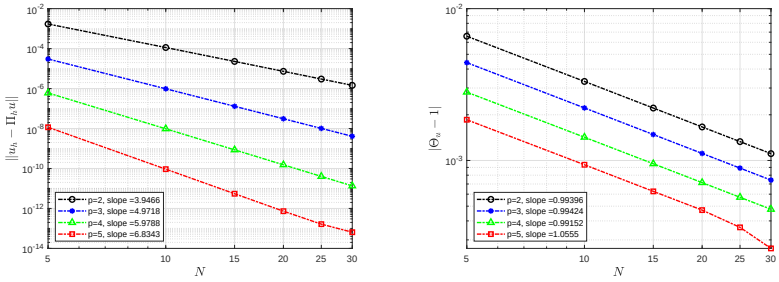

Figure 9: Convergence rates for $\|u_h - \Pi_h u\|$ (left) and $\|\Theta_u - 1\|$ (right) for the BVP (77) on uniform meshes having $N = 5$, 10, 15, 20, 25, 30 elements using $p =$ 2-5.

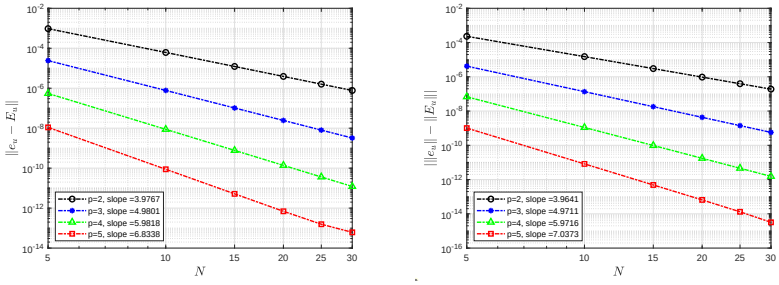

Figure 10: Convergence rates for $\|e_u - E_u\|$ (left) and $|\|e_u\| - \|E_u\||$ (right) for the BVP (77) on uniform meshes having $N = 5$, 10, 15, 20, 25, 30 elements using $p =$ 2-5.

Example 5.4. In the last example, we consider the following BVP

$$u'' - \ln(1+u^2) = e^x - \ln(1+2^{2x}), \quad x \in [0,3], \quad u(0) = 1, \quad u'(3) = e^3, \tag{78}$$

where the exact solution is $u(x) = e^x$. In this example $f(x,u) = \ln(1+u^2) + e^x - \ln(1+2^{2x})$, which satisfies the assumptions used in our theorems. We use the uniform mesh with $N = 4$, 8, 12, 16, 20, 24 elements. The results in the left figure of Figure 11 clearly show that $\|u_h - \Pi_h u\| = \mathcal{O}(h^{p+2})$. From the results shown in the left figure of Figure 12 it is clear that $\|e_u - E_u\| = \mathcal{O}(h^{p+2})$. The results shown in the right figure of Figure 12 again demonstrate that $|\|e_u\| - \|E_u\|| = \mathcal{O}(h^{p+2})$ as $h \to 0$. Thus, our *a posteriori* error estimate E_u converges to the actual error e_u as $h \to 0$. The global effectivity indices Θ_u presented in Table 8 indicate that Θ_u is near unity and converges to one under h-refinement. Finally, the results presented in the right figure of Figure 11 suggest that $|\Theta_u - 1| = \mathcal{O}(h)$. Thus, the numerical convergence rates are sharp.

TABLE 8. Global effectivity indices for Example 5.4 on uniform meshes having $N = 4$, 8, 12, 16, 20, 24 elements using $p = 2 - 5$.

$p \backslash N$	$N = 4$	$N = 8$	$N = 12$	$N = 16$	$N = 20$	$N = 24$
$p = 2$	1.0125	1.0052	1.0032	1.0023	1.0018	1.0015
$p = 3$	1.0080	1.0034	1.0021	1.0015	1.0012	1.0010
$p = 4$	1.0048	1.0021	1.0013	1.0010	1.0008	1.0006
$p = 5$	1.0031	1.0013	1.0009	1.0006	1.0005	1.0004

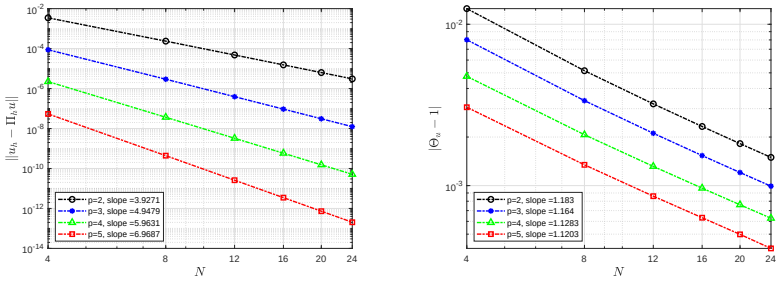

Figure 11: Convergence rates for $\|u_h - \Pi_h u\|$ (left) and $\|\Theta_u - 1\|$ (right) for the BVP (78) on uniform meshes having $N = 4$, 8, 12, 16, 20, 24 elements using $p =$ 2-5.

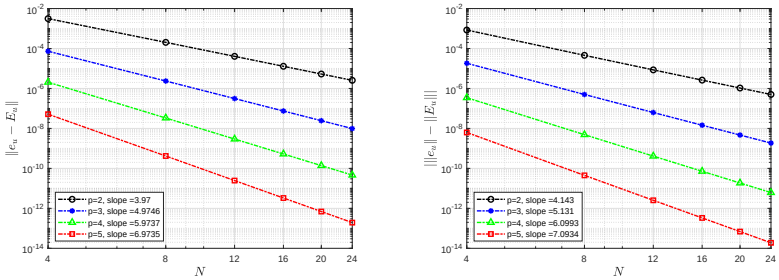

Figure 12: Convergence rates for $\|e_u - E_u\|$ (left) and $|\|e_u\| - \|E_u\||$ (right) for the BVP (78) on uniform meshes having $N = 4$, 8, 12, 16, 20, 24 elements using $p =$ 2-5.

6. Concluding remarks

In this paper, we developed and analyzed an *a posteriori* error estimator for the ultra-weak discontinuous Galerkin (UWDG) method for nonlinear boundary-value problems of the form $u'' = f(x, u)$ with suitable boundary conditions. We first proved that the dominant part of the discretization error for the p-degree UWDG solution is proportional to a $(p + 1)$-degree polynomial. We used these results to construct asymptotically exact *a posteriori* error estimates. The proposed *a posteriori* error estimator is computationally simple, efficient, and asymptotically exact. This estimator is obtained by solving a local residual problem on each element. The proposed *a posteriori* error estimate is shown to converge to the actual error in the L^2-norm under mesh refinement. The order of convergence is proved to be $p + 2$, when piecewise polynomials of degree $p \geq 2$ are used. Our numerical experiments demonstrate that the results in this paper hold true for nonlinear problems with general function $f(x, u)$, indicating that the restriction on $f(x, u)$ is artificial. The generalization of our proofs to nonlinear equations with general function f involves several technical difficulties and will be investigated in the future. We are currently investigating the superconvergence properties and the asymptotic exactness of *a posteriori* error estimates for UWDG methods applied to two-dimensional elliptic, parabolic, and hyperbolic equations on rectangular and triangular meshes. Our future work will focus on extending our *a posteriori* error analysis to linear and nonlinear problems on tetrahedral meshes.

Conflict of interest: The author declares no conflict of interest.

Ethical statement: The author agrees that this manuscript has followed the rules of ethics presented in the journal's Ethical Guidelines for Journal Publication.

Acknowledgements: The author would like to thank the two anonymous reviewers for the valuable comments and suggestions which improved the quality of the paper.

Funding: This research was partially supported by the NASA Nebraska Space Grant (Federal Grant/Award Number 80NSSC20M0112) and by the University Committee on Research and Creative Activity at the University of Nebraska at Omaha.

References

[1] M. Abramowitz and I. A. Stegun. *Handbook of Mathematical Functions*. Dover, New York, 1965.

[2] S. Adjerid and M. Baccouch. Asymptotically exact *a posteriori* error estimates for a one-dimensional linear hyperbolic problem. *Applied Numerical Mathematics*, 60:903–914, 2010.

[3] M. Ainsworth and J. T. Oden. A posteriori *Error Estimation in Finite Element Analysis*. John Wiley, New York, 2000.

[4] A. Aziz. *Numerical Solutions of Boundary Value Problems for Ordinary Differential Equations*. Academic Press, 1975.

[5] I. Babuška and T. Strouboulis. *The Finite Element Method and Its Reliability*. Numerical mathematics and scientific computation. Clarendon Press, 2001.

[6] I. Babuška, R. Durán, and R. Rodríguez. Analysis of the efficiency of an a posteriori error estimator for linear triangular finite elements. *SIAM journal on numerical analysis*, 29(4):947–964, 1992.

[7] M. Baccouch. A superconvergent ultra-weak discontinuous Galerkin method for nonlinear second-order two-point boundary-value problems. *Journal of Applied Mathematics and Computing*, 69:1507–1539, 2023.

[8] R. L. Burden, J. D. Faires, and A. M. Burden. *Numerical analysis*. Cengage Learning, Boston, MA, 2016.

[9] M. Chawla and C. Katti. Finite difference methods for two-point boundary value problems involving high order differential equations. *BIT Numerical Mathematics*, 19(1):27–33, 1979.

[10] P. G. Ciarlet. *The finite element method for elliptic problems*. SIAM, 2002.

[11] B. Cockburn, S.-Y. Lin, and C.-W. Shu. TVB Runge-Kutta local projection discontinuous Galerkin finite element method for conservation laws III: One dimensional systems. *Journal of Computational Physics*, 84:90–113, 1989.

[12] B. Cockburn and C. W. Shu. TVB Runge-Kutta local projection discontinuous Galerkin methods for scalar conservation laws II: General framework. *Mathematics of Computation*, 52:411–435, 1989.

[13] B. Cockburn and C. W. Shu. The local discontinuous Galerkin method for time-dependent convection-diffusion systems. *SIAM Journal on Numerical Analysis*, 35:2440–2463, 1998.

[14] B. Cockburn and C.-W. Shu. The Runge-Kutta discontinuous Galerkin method for conservation laws V: multidimensional systems. *Journal of Computational Physics*, 141:199–224, 1998.

[15] C. De Coster and P. Habets. *Two-Point Boundary Value Problems: Lower and Upper Solutions*. Mathematics in Science and Engineering. Elsevier, 2006.

[16] B. Despres. Sur une formulation variationnelle de type ultra-faible. *Comptes rendus de l'Académie des sciences. Série 1, Mathématique*, 318(10):939–944, 1994.

[17] B. Dong and C.-W. Shu. Analysis of a local discontinuous Galerkin method for linear time-dependent fourth-order problems. *SIAM Journal on Numerical Analysis*, 47:3240–3268, 2009.

[18] H. B. Keller. *Numerical Methods for Two-point Boundary-value Problems*. A Blaisdell Book in Numerical Analysis and Computer Science. Blaisdell, Waltham, MA, 1968.

[19] W. H. Reed and T. R. Hill. Triangular mesh methods for the neutron transport equation. Technical Report LA-UR-73-479, Los Alamos Scientific Laboratory, Los Alamos, 1973.

[20] L. Schumaker. *Spline functions: basic theory*. Cambridge University Press, Cambridge New York, 2007.

[21] K. Segeth. *A posteriori* error estimation with the finite element method of lines for a nonlinear parabolic equation in one space dimension. *Numerische Mathematik*, 83(3):455–475, 1999.

[22] Q. Tao, Y. Xu, and C.-W. Shu. An ultraweak-local discontinuous Galerkin method for PDEs with high order spatial derivatives. *Mathematics of Computation*, 89(326):2753–2783, 2020.
[23] R. Verfürth. *A posteriori* error estimation and adaptive mesh-refinement techniques. *Computational and Applied Mathematics*, 50:67–83, 1994.
[24] L. Wahlbin. *Superconvergence in Galerkin finite element methods*. Lecture notes in mathematics. Springer, 1995.
[25] Y. Xu and C.-W. Shu. Optimal error estimates of the semi-discrete local discontinuous Galerkin methods for high order wave equations. *SIAM Journal on Numerical Analysis*, 50:79–104, 2012.
[26] J. Yan and C.-W. Shu. A local discontinuous Galerkin method for KdV type equations. *SIAM Journal on Numerical Analysis*, 40:769–791, 2002.

Department of Mathematics, University of Nebraska at Omaha, Omaha, NE 68182, USA
E-mail: mbaccouch@unomaha.edu